

# PCCP

Accepted Manuscript



This is an *Accepted Manuscript*, which has been through the Royal Society of Chemistry peer review process and has been accepted for publication.

*Accepted Manuscripts* are published online shortly after acceptance, before technical editing, formatting and proof reading. Using this free service, authors can make their results available to the community, in citable form, before we publish the edited article. We will replace this *Accepted Manuscript* with the edited and formatted *Advance Article* as soon as it is available.

You can find more information about *Accepted Manuscripts* in the [Information for Authors](#).

Please note that technical editing may introduce minor changes to the text and/or graphics, which may alter content. The journal's standard [Terms & Conditions](#) and the [Ethical guidelines](#) still apply. In no event shall the Royal Society of Chemistry be held responsible for any errors or omissions in this *Accepted Manuscript* or any consequences arising from the use of any information it contains.

# Global Investigation of Potential Energy Surfaces for the Pyrolysis of C<sub>1</sub>-C<sub>3</sub> Hydrocarbons: Toward the Development of Detailed Kinetic Models from First Principles

Mikhail N. Ryazantsev,<sup>1†</sup> Adeel Jamal,<sup>1†</sup> Satoshi Maeda,<sup>2</sup> and Keiji Morokuma<sup>1,3\*</sup>  
mikhail.n.ryazantsev@gmail.com, adeel.jamal@gmail.com, smaeda@mail.sci.hokudai.ac.jp,  
[keiji.morokuma@emory.edu](mailto:keiji.morokuma@emory.edu)

<sup>1</sup>Department of Chemistry and Cherry L. Emerson Center for Scientific Computation, Emory University, Atlanta, Georgia 30322

<sup>2</sup>Department of Chemistry, Faculty of Science, Hokkaido University, Sapporo 060-0810, Japan

<sup>3</sup>Fukui Institute for Fundamental Chemistry, Kyoto University, Kyoto 606-8103, Japan

<sup>†</sup>Contributed equally to this work

\*Corresponding Author:

Professor Dr. Keiji Morokuma; Email: [morokuma@fukui.kyoto-u.ac.jp](mailto:morokuma@fukui.kyoto-u.ac.jp);  
[keiji.morokuma@emory.edu](mailto:keiji.morokuma@emory.edu); Phone: +81-75-711-7843

### Abstract

Detailed kinetic models (DKM) are the most fundamental “bottom-up” approach to computational investigation of the pyrolysis and oxidation of fuels. The weakest points of existing DKM are incomplete information about the reaction types that can be involved in the potential energy surfaces (PES) in pyrolysis and oxidation processes. Also, the computational thermodynamic parameters available in the literature vary widely with the level of theory employed. More sophisticated models require improvement both in our knowledge of the type of the reactions involved and the consistency of thermodynamic and kinetic parameters. In this paper, we aim to address these issues by developing ab initio models that can be used to describe early stages of pyrolysis of C<sub>1</sub>-C<sub>3</sub> hydrocarbons. We applied a recently developed Global Reaction Route Mapping (GRRM) strategy to systematically investigate the PES of the pyrolysis of C<sub>1</sub>-C<sub>3</sub> hydrocarbons at a consistent level of theory. The reactions are classified into 14 reaction types. The critical points on the PES for all reactions in the network are calculated at the highly accurate UCCSD(T)-F12b/cc-pVTZ//UM06-2X/cc-pVTZ level of theory. The data reported in this paper can be used for first principle calculations of kinetic constants and for a subsequent study on modeling the evolution of the species from the reaction network of the pyrolysis and oxidation of C<sub>1</sub>-C<sub>3</sub> hydrocarbons.

## 1. Introduction

Gasoline, diesel and jet fuels are generally composed of hundreds to thousands of compounds. For fuels derived from petroleum sources, majority of these compounds are different types of hydrocarbons with variety of functional groups and carbon chain length.<sup>1,2</sup> Therefore, studies of combustion processes for such fuels require robust pyrolysis and combustion models for different kind of hydrocarbons. The combustion processes at the molecular level even for the simplest hydrocarbons remains an active area of study. Recent developments in both experimental and theoretical methodologies allow for improvements of pyrolysis and combustion models.

Recent progress in time-resolved measurements has been accomplished by combining shock tube experiments with laser diagnostics.<sup>3</sup> Flexibility of shock tube experiments combined with non-intrusive, species-specific, quantitative laser diagnostic allows for high quality measurement of ignition delay times, species time histories, and elementary reaction rates in large temperature and pressure range.<sup>3-7</sup> These sophisticated experimental measurements provide a reliable basis for validations of computational models. In particular, these experimental techniques can provide time-resolved concentration profiles for multiple species and, therefore, enable to test the performance of various models at different stages of combustion processes – from very initial stages of pyrolysis and oxidation to advanced stages that include many complicated processes such as soot formation. Recently, several time-resolved studies have been reported that question the quality of widely used combustion models.<sup>8-10</sup> These studies motivate further improvements of existing computational models.

A number of techniques are used to model combustion processes. They range from computational fluid dynamics where fuel hydrodynamics is the focus of study, to detailed chemical models where the chemistry of the combustion process is the primary object of interest.<sup>11-15</sup> In principle, kinetic models based on elementary reactions are the most fundamental “bottom-up” approach to combustion modeling.<sup>14-17</sup> A detailed model obtained from fundamental chemical principles and validated by experiments can be used as a basis for further implementation into the models of real engines at a specific set of conditions.<sup>18</sup> Several points that are important to construct a robust detailed kinetic model from first principles must be considered:

1. Combustion chemistry is often very complex, and a reaction network generally involves dozens to hundreds of species and hundreds to thousands of reactions steps.<sup>17,19</sup> To generate the reaction network for a combustion model, one has to specify reaction species and types. Still, prediction of all chemical reaction types that are involved in the process is not trivial, and some important reaction types may not be included in existing models. For example, even for a relatively simple process such as initial steps of pyrolysis of hydrocarbons, new roaming reaction types have been reported recently.<sup>20,21</sup> A global investigation must be performed to incorporate all reaction steps for that particular reaction type. Similarly, new reaction steps have been found in thermal decomposition of dimethyl ether.<sup>2</sup> To include all important reaction steps into a model, a global investigation of all possible reaction paths, i.e. a systematic global investigation of the potential energy surface, is required in establishing a reaction network.
2. A large number of parameters required to build a detailed kinetic model does not provide unbiased evaluation of these parameters based on fitting experimental data. To overcome this obstacle and limit the number of parameters to fit, group additivity models and group contribution methods (or structure-relativity relationships) have been used for thermodynamic and kinetic parameters, respectively.<sup>23-29</sup> In addition, empirical parameters to describe intermolecular energy transfer<sup>30-33</sup> and, if necessary, rate constants for radiationless electronic transitions have to be included in a model.<sup>34</sup> Once the model is generated and most sensitive parameters for a specific target experiment are identified, these parameters can be tuned to fit target experiments.<sup>35-38</sup> Still, implementation of these methodologies for complex reaction networks remains challenging, and the above-mentioned techniques for estimation of thermodynamic and kinetic parameters do not always provide sufficient quality to build a robust model. Direct experimental determination of thermodynamic parameters and rate constants for all reactions in a model is hardly possible. In principle, modern computational chemistry allows for evaluation of both thermodynamic and kinetic parameters that are shown to be in very good agreement with parameters obtained from experiment.<sup>34,39-48</sup> Therefore, parameters calculated from first principles can considerably improve a kinetic model. Although the number of successful implementations of computational chemistry to elementary processes relevant to combustion chemistry are enormous, still, full ab initio investigations of complex

reaction networks are not so common.<sup>49</sup> One of the impeding factors for more extensive implementation of computational chemistry to combustion models is the large number of elementary processes that are involved in combustion processes and, therefore, a large number of calculations of the critical points (i.e. local minima and saddle points) on potential energy surfaces has to be done. Furthermore, the available data in the literature are presented in a variety levels of theory. Depending on the level or basis set employed, certain critical points may vary in structure and energy from one level of theory to another. In the most extreme case, certain reaction steps may be neglected altogether from one study to another. Thus, it is critical that a consistent level of theory is applied in obtaining all of the thermodynamic and kinetic parameters in the systematic development of a kinetic model.

3. A reaction network can become manually intractable with the growth of the number of atoms for species involved in the process (both for combustion of bigger compounds and because of chain-growth reactions on longer time scale). In this case, automatic reaction network generators are limited to the species and types of reactions in their database. A consequence of this is that novel reaction species, reaction types, and elementary reaction steps may be excluded in the reaction network.<sup>27,29,50-53,78-79</sup> This may include contributions from the excited state potential energy surfaces.

Recently, we have developed a tool for global exploration of potential energy surface: global reaction route mapping (GRRM) strategy, an automated search method for reaction pathways starting from a given set of the reactants.<sup>54-57</sup> GRRM methodology consists of two independent complementary methods: anharmonic downward distortion following (ADDF) and artificial force induced reaction (AFIR) methods. ADDF can follow reaction pathways starting from local minima on the potential energy surface (PES) through transition structures (TSs) to isomerization and dissociation products. AFIR can find pathways starting from two or more reactants toward TSs for their associative reactions. In other words, ADDF searches for  $A \rightarrow X$  type isomerization and  $A \rightarrow X + Y$  type dissociation pathways, whereas AFIR finds  $A + B \rightarrow X (+ Y)$  type pathways. In addition, both ADDF and AFIR methodologies (in conjunction with seam model function approach)<sup>58</sup> can be used to explore the topology (minima and saddle points) of seam-of-crossing and conical intersection hypersurface between two adiabatic potential energy surfaces.<sup>55</sup>

GRRM strategy can be useful to develop kinetic models from first principles to address the points stated above:

1. GRRM allows for an ab initio global investigation of the topology of PESs for species and reactions involved in pyrolysis and combustion processes without any a priori knowledge. Based on these calculations, the reactions that are energetically accessible under given conditions can be identified and included in a kinetic model.
2. Structures and energies of minima and TSs that are automatically obtained from the GRRM search can be used to calculate thermodynamic and kinetic parameters for reactions included in the reaction network. The global investigation is performed in a systematic manner at a consistent level of theory for all of the reaction types and elementary steps involved.
3. The automatic global exploration of the PESs allows feasibility for the number of reactions involved. This can be of great utility for the study of the pyrolysis and oxidation of larger hydrocarbons. Further, GRRM can also be used to automatically explore the excited potential energy surfaces and associated minimum energy points on seams of crossing where conical intersections (CI) and intersystem crossing (ISC) may occur.

In this paper, which is the first part of our studies, we report our GRRM investigation of the potential energy surfaces for closed-shell singlet and doublet species involved in the early stages of pyrolysis of C<sub>1</sub>-C<sub>3</sub> hydrocarbons as well as energetics of all of the reactions and transition states.<sup>16,17,59</sup> Similar investigation for triplet compounds and carbenes, calculations of kinetics constants, and evolution of the species for pyrolysis of specific compounds will be reported later. In addition, the pyrolysis of C<sub>1</sub>-C<sub>3</sub> hydrocarbons is widely investigated experimentally including shock tube/laser diagnostic techniques<sup>60</sup> and, therefore, a detailed kinetic model for pyrolysis of these compounds can be easily verified.

## 2. Theoretical methods

**Generation of the species used for GRRM search.** To keep the number of unimolecular and bimolecular reaction involved in our GRRM investigation tractable, in this paper the reactions that involve a reactant larger than C<sub>3</sub> were neglected. Therefore, any species in the reaction network do not exceed C<sub>6</sub>. The set of the species are given in Fig.1. The reaction set includes all unimolecular reactions for C<sub>1</sub>, C<sub>2</sub> and C<sub>3</sub> compounds and all bimolecular reactions between

them. The obtained model can be expected to be valid at least for initial stage of pyrolysis. On longer time scales, chain-growth reactions become important and the reaction network grows dramatically. Such large networks are hardly tractable manually and an automated network generator must be involved.<sup>27,50-53</sup> Therefore, chain-growth processes in industrial pyrolysis and combustion is out of scope of this study. In this article we report our investigation only for singlet and doublet potential energy surfaces for close-shell compounds and radicals, respectively. However, our results indicate that reactions on the triplet potential energy surfaces as well as reactions that involve singlet and triplet carbenes are energetically accessible and may contribute to the pyrolysis of unsaturated compounds. Therefore, these reactions should be investigated further.

--- Fig. 1 ---

**GRRM search.** We started from a set of species shown in Fig.1. The ADDF methodology was used to investigate PESs for unimolecular reactions for all species ( $A \rightarrow X$  type isomerization and  $A \rightarrow X + Y$  type dissociation). The AFIR methodology was used to investigate PESs for bimolecular reactions ( $A + B \rightarrow X (+ Y)$  type) between all possible pairs of species in Fig. 1. UM06-2X/6-31g\* level of theory<sup>61</sup> was used for both ADDF and AFIR search.

**Refinement of the critical points from GRRM search.** All minima and TSs structures obtained from GRRM search were re-optimized at the UM06-2X/cc-pVTZ level of theory.<sup>61</sup> Energies for minima and TSs structures were recalculated at the UCCSD(T)-F12b/cc-pVTZ//UM06-2X/cc-pVTZ + ZPE(UM06-2X/cc-pVTZ) level, which include the zero point energy (ZPE) correction at the UM06-2X/cc-pVTZ level. UCCSD(T)-F12b is a recently developed explicitly correlated coupled-cluster methods that yield RHF-UCCSD(T) results with near basis set limit accuracy already with double- $\zeta$  or triple- $\zeta$  basis sets.<sup>62,63</sup> The software packages Gaussian09<sup>64</sup> and MOLPRO2012<sup>65</sup> were used for the calculations.

### 3. Results and Discussion

Table S3 summarizes the full set of reactions studied, both unimolecular and bimolecular, with the reaction barrier heights and energies (with ZPE correction) and enthalpies of the reactions (in kcal/mol) at the UCCSD(T)-F12/cc-pVTZ//UM06-2X/cc-pVTZ level with vibration and rotational energies calculated at the UM06-2X/cc-pVTZ level. The enthalpies of the reactions are compared with experimental values from the gas-phase thermochemistry data in the

Webbook of the National Institute of Standards and Technology (NIST) database.<sup>66</sup> The values obtained from NIST and Active Thermochemical Tables (ATcT)<sup>80</sup> are given in Table S2 of the ESI and deviations between NIST and ATcT values are also provided. The reactions are classified into reaction types and are discussed in detail in the following subsections

---Table S3 ---

### 3.1 Reaction Type 1: Unimolecular C-H Bond Dissociation in Closed Shell Species

The C-H bond dissociation in closed-shell species occurs barrierlessly and results in a radical and an H atom. The energy required to break a C-H bond correlates with the stability of resulting radicals as is shown in Fig 2. The more stable the resultant radical species, the lower the dissociation energy. The highest energies of C-H bond dissociation (around 130 kcal/mol) are required for cleavage of a H-C(sp) bond to create an unstable radical such as  $\text{CH}_3\text{C}\equiv\text{C}$  (1-propynyl) and  $\text{CH}\equiv\text{C}$  (ethynyl), followed by around 110 kcal/mol for cleavage of a H-C(sp<sup>2</sup>) bond and around 100 kcal/mol for cleavage of a H-C(sp<sup>3</sup>) bond. The lowest energies (around 90 kcal/mol) are for cleavage of a H-C(sp<sup>3conj</sup>) bond creating radicals stabilized by  $\pi$ -conjugation  $\text{CH}_2\text{-CH=CH}_2$  (allyl),  $\text{CH}_2\text{=C=CH}$  and  $\text{CH}_2\text{-C}\equiv\text{CH}$  (propargyl), denoted as  $\pi\text{-C}$  in Fig 2 and Fig 3. For cyc- $\text{CH}_2\text{CH=CH}$ , the bond dissociation energies for the H-C(sp<sup>3conj</sup>) and H-C(sp<sup>2</sup>) bond cleavage are 99 and 108 kcal/mol, respectively, close to the dissociation energies for H-C(sp<sup>3conj</sup>) and H-C(sp<sup>2</sup>) in non-cyclic compounds. On the contrary, the H-C(sp<sup>3</sup>) bond dissociation energy from cyc- $\text{CH}_2\text{CH}_2\text{CH}_2$  is 42 kcal/mol, which is about 60 kcal/mol lower than the H-C(sp<sup>3</sup>) dissociation energy for non-cyclic compounds, indicating that a large strain energy is released by the H-C bond cleavage in this compound.

--- Fig. 2 ---

For propane and ethane, the energies of C-H bond cleavage are about 10 kcal/mol higher than the energies that are required for C-C bond cleavage. Therefore, for alkanes investigated in this study, C-H bond cleavage is the energetically most favorable process only for the initial step of methane pyrolysis. For alkenes in Fig. 1, breaking any bond between two carbons is energetically less favorable than C-H bond cleavage. However, for these species, H-transfer forming carbenes and/or conversion to triplet state with a subsequent C-C bond cleavage on the triplet potential energy surface are competitive processes as described later.

### 3.2 Reaction Type 2: Unimolecular C-C Bond Dissociation in Closed Shell Species.

The dissociation of a C-C single bond in closed-shell species occurs barrierlessly and results in two radicals. Generally, the energy required for breaking a single bond between two carbons correlates with stability of the radicals that are produced in the reaction. This correlation is demonstrated in Fig 3. Fig. 3 also includes the energies for type 11 reactions: bimolecular radical recombination reactions, which are reverse reactions of type 2 (reactions from t11-2-1 to t11-16-1 in table S3). The highest energies of C-C bond dissociation (around 160 kcal/mol) are required for cleavage of a C(sp)-C(sp) bond to create two R≡C radicals. The next is about 130-140 kcal/mol for creation of one R≡C radical and one R<sub>2</sub>C=CR radical from C(sp)-C(sp<sup>2</sup>) bond, then about 120 kcal/mol for C(sp)-C(sp<sup>3</sup>) bond, about 110 kcal/mol for C(sp)-C(sp<sup>3conj</sup>) bond and for C(sp<sup>2</sup>)-C(sp<sup>2</sup>) bond, about 90-100 kcal/mol for a C(sp<sup>2</sup>)-C(sp<sup>3</sup>) bond, about 80-90 kcal/mol for C(sp<sup>3</sup>)-C(sp<sup>3</sup>) bond and C(sp<sup>2</sup>)-C(sp<sup>3conj</sup>) bond, and about 70-80 kcal/mol for C(sp<sup>3</sup>)-C(sp<sup>3conj</sup>) bond. The lowest bond dissociation energy is about 60-70 kcal/mol for the C(sp<sup>3conj</sup>)-C(sp<sup>3conj</sup>) bond producing two conjugated sp<sup>2</sup> radicals.

--- Fig. 3 ---

These results indicate that a single C-C bond cleavage, requiring about 80-90 kcal/mol, has the lower energy demand than the C-H bond cleavage. Therefore, the C-C bond cleavage is the most important initiation process for the decomposition of alkanes. For ethane and propane, the C-C dissociation process requiring 88.2 and 87.2 kcal/mol, respectively, is more favorable than the C-H dissociation requiring 99.9 and 97.0 kcal/mol, respectively. Energies of dissociation of C=C double and C≡C triple bonds are much higher than the energy of a C-C single bond (t2-3, -5, -6 and -8 in Table S3). Therefore, decomposition of simple alkenes and alkynes does not involve a direct cleavage of double or triple bonds but occurs via other lower energy processes such as single C-C or C-H bond cleavage, H transfer or via reactions on the triplet potential energy surface, as discussed in section 3.5 (reaction type 5: Unimolecular H-transfer in Unsaturated Closed Shell Species, and 3.9 reaction type 9: Singlet to Triplet Crossings for Closed Shell and Carbene Species)

### 3.3 Reaction Type 3: Unimolecular Double C-H Bond Cleavage in Closed Shell Species

Double C-H bond cleavages from a closed-shell species occur via a transition state that involves two C-H bond cleavages, followed by an H-H bond formation. Both C-H bond cleavages can occur on the same carbon, resulting in a carbene and a hydrogen molecule, or they can occur on adjacent carbons, resulting in the formation of closed-shell species with a double bond and a hydrogen molecule. There are two pathways for the reaction  $\text{CH}_3\text{CH}_2\text{CH}_3 \rightarrow \text{CH}_3\text{CH}=\text{CH}_2 + \text{H}_2$ , (t3-5) and (t3-6). As shown in Fig. 4, snapshots from IRC following for (t3-5) with the barrier of 104.1 kcal/mol indicate that the reaction takes place asynchronously; namely, one of the terminal hydrogen of propane starts to dissociate, which then attracts one of the central  $\text{CH}_2$  hydrogens to form a hydrogen molecule as they dissociate leaving the stable  $\text{CH}_3\text{CH}=\text{CH}_2$  behind. Snapshots for (t3-6) with the barrier of 110.4 kcal/mol, on the other hand, show a very different pathway; two hydrogen atoms from two terminal carbons start to dissociate simultaneously and form a hydrogen molecule, which is followed by a transfer of a hydrogen atom from the central carbon to a terminal carbon, to result in  $\text{CH}_3\text{CH}=\text{CH}_2$ , the same stable product as in (t3-5).

--- Fig. 4 ---

The energy of the reactions which results in a carbene formation is about 60 kcal/mol higher than the energy of the reactions which leads to formation of a closed shell unsaturated species. The formation of methylene carbenes ( $\text{R}=\text{C}$ ) is lower in energy by about 20 kcal/mol than the formation of methyl carbenes ( $\text{R}-\text{CH}$ ).

### 3.4 Reaction Type 4: Unimolecular Simultaneous C-C and C-H Bond Cleavage in Closed Shell Species

The simultaneous C-C and C-H bond cleavage in closed-shell species occurs through a transition state. Along the reaction pathway, an initial C-C bond cleavage that produces two alkyl radicals follows by an H-atom abstraction by one alkyl radical from the other alkyl radical leading to either two closed shell products or a carbene and a closed shell product. As shown in Table S3, from propane three lower energy pathways all produce methane and ethylene. As shown in Fig. 5, the lowest path t4-4, is a direct concerted path in which the dissociating  $\text{CH}_3$  fragment abstracts a hydrogen atom from the  $\text{CH}_3$  group of the ethyl radical to produce ethylene and methane. Slightly (4.0 kcal/mol) higher in energy is the path t4-2, in which the dissociated  $\text{CH}_3$  becomes planar with respect to the nascent ethyl radical, then abstracts an H-atom from

ethyl radical to also produce ethylene and methane. The highest energy path, t4-3, where the dissociated  $\text{CH}_3$  from propane rotates non-planar to the nascent ethyl radical, and abstracts a hydrogen atom to also form ethylene and methane. An alternate unimolecular simultaneous C-C and C-H bond cleavage occurs with reaction steps t4-5 and t4-6. For the former reaction step, t4-5, a C-C bond cleavage occurs, generating ethyl and methyl radicals also, but an H-abstraction occurs by the ethyl radical from the methyl radical, producing ethane and  $^1\text{CH}_2$ . For reaction step t4-6, a similar C-C bond cleavage as described in t4-2, t4-3, t4-4, and t4-5 also occurs. Here instead, it involves an H-atom abstraction from by methyl radical from the  $\text{CH}_2$  fragment of ethyl radical, producing ethyl carbene and methane.

The energies of the transition states for t4-5 and t4-6 are reported in Table S4 of the ESI, where energies of the MRCI+Q-F12/cc-pVTZ//UM06-2X/cc-pVTZ + ZPE(UM06-2X/cc-pVTZ) calculations (given as TSb) were also calculated for comparison to the UCCSD(T)-F12b/cc-pVTZ//UM06-2X/cc-pVTZ energies (given as Tsa) used in this study. Calculations of T1 diagnostic values from the UCCSD(T)-F12b/cc-pVTZ//UM06-2X/cc-pVTZ for the transition states of t4-5 and t4-6 were also reported in table S4, with values below 0.02, indicating no strong multi-reference character in the wavefunctions for these transition states. In comparison to G2M(CC2)<sup>81</sup> energies, the energy of the transition state for t4-5 deviated by 2.4 kcal/mol while the energy of transition state for t4-6 deviated by 0.5 kcal/mol.<sup>82</sup>

Finally, we found a simultaneous C-C bond cleavage followed by a C-H bond abstraction path for propene decomposition (reaction t4-8 in table S3 and Figure 6). Here, C-C bond cleavage results in two nascent radicals,  $\text{CH}_3$  and  $\text{CH}_2=\text{CH}$ , followed by H-abstraction by  $\text{CH}_2=\text{CH}$  from the methyl radical, forming carbene  $^1\text{CH}_2$  and  $\text{CH}_2=\text{CH}_2$ , which then a  $\text{CH}_2$  addition to the double bond of ethylene occurs, forming cyclopropane. A C-C roaming path for propene decomposition that leads to  $\text{CH}_4 + \text{CH}\equiv\text{CH}$  could not be located at the UM06-2X/cc-pVTZ level of theory. This may be from the rigidity of the propene molecule, where the nascent  $\text{CH}_3$  radical must abstract the H-atom from the other terminal site of propene.

Some of these “roaming” type reactions have been recently reported to make a small but detectable contribution to the initial step of alkane pyrolysis.<sup>21,22</sup> However, further theoretical and experimental investigations are needed for better understanding of the role of this reaction type in pyrolysis and combustion of hydrocarbons.

--- Fig. 5 ---

Generally, reactions of this type are energetically less favorable than competing reactions such as C-C bond cleavage for alkanes and conversion to the triplet state and/or unimolecular H-transfer for alkenes. Further, roaming radical mechanism can be thought of a pathway in a shallow valley of the PES connecting the weak-complex of disproportionation reactions to the radical recombination products (described in Sec. 3.14). Thus, there may exist certain trajectories that may not have been located in these flat regions of the PES at the UM06-2X/cc-pVTZ level of theory. Further multi-reference studies may be better suited for these reaction steps.

### 3.5 Reaction Type 5: Unimolecular H-transfer in Unsaturated Closed Shell Species

An H-transfer in unsaturated closed-shell species between carbon atoms occurs through a transition state resulting in formation of carbenes. For ethylene and acetylene, only 1,2 H-transfer is possible (t5-1, t5-2, t5-6, t5-7 in table S3). For propene and propyne, 1,3 H-transfer is also possible. As a rule, primary carbenes and diradicals that form in these reactions are not very stable and, in several cases, the corresponding minima on potential energy surface do not exist. Thus, the minimum energy path for 1,2 H-transfer in propene (reaction t5-5 in table S3 and Figure 6) does not feature any stable diradical intermediate but directly leads via a diradical-like transition state to cyclopropane. However, it must be noticed that a very shallow minimum for the diradical structure was located at the UMP2/6-31G\*\* level of theory in a previous study<sup>67</sup> (as well as a transition state structure that is similar to the TS structure reported in our study). This dependence on the level of theory used is a common feature for these type of primary carbenes and diradicals. Similarly, we were not able to locate a minimum for CH<sub>3</sub>CH<sub>2</sub>CH carbene at the UM06-2X/cc-pVTZ level of theory (but at UB3LYP/3-21g the minimum was found). The secondary carbene CH<sub>3</sub>CCH<sub>3</sub> was found to be relatively stable (reactions t5-3 and t5-4 in table S3). In contrary to propyne, 1,3 H-transfer in propene leads to the same compound, propene, and this reaction is not considered in this study.

One of the possible 1,2 H-transfers in propyne results again in cyclization (reaction t5-9 in table S3 and Figure 6). In this reaction, an initial 1,2 H-transfer is followed by another 1,3 H-transfer to form cyclopropene. The second possible 1,2 H-transfer in propyne produces a carbene, CH<sub>2</sub>=CHCH (reactions t5-10 and t5-11 in table S3). The transition state region for this reaction is extremely flat and located very closed to the product. For this reason, we were not

able to locate it and the energy of the product is used for transition state in table S3. Finally, 1-3 H-transfer in propyne gives allene (reactions t5-11 and t5-12 in table S3).

Generally, unimolecular H-transfer in unsaturated closed shell species forming carbenes is the kinetically most favorable route for the initial decomposition of alkynes and the kinetically most favorable routes on the singlet potential energy surface for the initial decomposition of alkenes. However, the barriers for the reverse reactions, H-transfer in carbenes to form unsaturated hydrocarbons, are much lower than the barriers for direct reactions (except the reaction t5-1:  $\text{CH}_2=\text{CH}_2 \rightarrow \text{CH}_3\text{CH}$ ), and, therefore, population of carbenes will be very low in equilibrium. On the other hand, singlet carbenes that are produced in these reactions are very reactive, and, in addition, can easily be converted to cyclic compounds or go through intersystem crossing to access the triplet potential energy surface (see table S3, Reaction Type 9). Including this reaction types into a kinetic model can be crucial to accurately describe pyrolysis and combustion of hydrocarbons. For instance, formation of singlet vinylidene,  $\text{CH}_2=\text{C}$  is suggested to be the main initial step of acetylene pyrolysis below 1300K<sup>68-70</sup>, in contrary to the radical mechanisms such as formation of vinyl and ethynyl radicals via disproportionation of two acetylene molecules<sup>68,71</sup> or formation of excited state acetylene biradical<sup>72,73</sup> as it was proposed before. Our reported barrier height of 0.9 kcal/mol from vinylidene-acetylene isomerization is in good agreement with the 1.3 kcal/mol barrier height reported in ultraviolet photoelectron spectroscopy studies<sup>78</sup> and the 1.5 kcal/mol barrier height reported couple-cluster calculations.<sup>79</sup>

In general, the reaction steps that involves  $\text{C}_1$ - $\text{C}_3$  carbenes and carbynes are not included in this report due to a relatively large reaction network that results with these reactants. The reactions with these species, which includes the triplet and possibly the excited state singlet potential energy surfaces, will be published later in a subsequent study. However, in this work we have shown that carbenes can easily be formed in pyrolysis of hydrocarbons, requiring a more detailed investigation that includes these reactions.

### 3.6 Reaction Type 6: Unimolecular C-H Bond Cleavage in Radical Species

The C-H bond cleavage of radical species results in an unsaturated closed-shell species and a hydrogen atom through a transition state, or a carbene species and a hydrogen atom through a barrierless process. The reactions that produce close shell compounds are much more kinetically

and thermodynamically favorable than the reactions that result in carbenes. Therefore, the formation of carbenes through this reaction type can be neglected in a detailed kinetic model.

The main competitive unimolecular route for this reaction type is the unimolecular C-C bond cleavage in radical species (reaction type 7). Similarly to C-C and C-H bond cleavage in alkanes,  $\beta$ -scission reactions, i.e. reactions that involve C-C bond cleavage to form unsaturated closed-shell compounds, are kinetically preferable over C-H bond cleavage reaction. However, for  $\text{CH}_3\text{CH}_2$  radical, where  $\beta$ -scission cannot occur, the C-H bond cleavage to form  $\text{CH}_2=\text{CH}_2$  (reaction t6-2) is the most preferable unimolecular process.

### 3.7 Reaction Type 7: Unimolecular C-C Bond Cleavage in Radical Species

Unimolecular C-C bond cleavage in radical species can be divided in two classes. The  $\beta$ -scission reactions that can occur in alkyl and alkenyl radicals with at least three carbon atoms produce a close shell unsaturated compound and a radical through a transition state. These reactions were shown to contribute to the pyrolysis and oxidation of hydrocarbons at relatively high temperatures ( $T \geq 850$ ).<sup>74,75</sup> The second class for this reaction type is a C-C bond cleavage that leads to a carbene and a radical species. These reactions have much higher barriers than  $\beta$ -scission reactions and do not contribute to the process.

### 3.8 Reaction Type 8: Unimolecular H-transfer in Radical Species

An H atom can be transferred from one site of a radical to another via a transition state. The mechanisms of these reactions are well-known and summarized.<sup>23</sup> For saturated species with three carbons, the transition state of a 1,2-H transfer of a  $\text{C}(\text{sp}^3)\text{-C}(\text{sp}^2)$  from an  $\text{sp}^3$ -carbon atom (such as cyc-CHCHCH) to an  $\text{sp}^2$ -carbon atom (cyc- $\text{CH}_2\text{CCH}$ ) is about 9 kcal/mol higher than the reverse process, an  $\text{sp}^2$ -carbon atom to an  $\text{sp}^3$ -carbon atom. The energy of the barriers for these reactions is relatively low and this type of the reaction should be considered in detailed kinetic models.

Similar  $\text{CH}_3$  transfer in any  $\text{C}_3$  radical results in the same  $\text{C}_3$  radical due to symmetry, and, for this reason, this reaction type is not considered in this study.

### 3.9 Reaction Type 9: Singlet to Triplet Crossings for Closed Shell and Carbene Species

Unimolecular singlet and triplet conversion via intersystem crossing both for closed-shell and carbene species is an important process that has to be considered for proper description of pyrolysis and oxidation of hydrocarbons. In recently published paper on propene pyrolysis, the singlet/triplet intersystem crossing for propene has been reported as the energetically lowest route.<sup>76</sup> In Table S3, we list the energies of the minima of triplet states relative to those of the minima on the singlet state. Our study confirms this finding but also suggests a more detailed investigation of H-transfer process that forms a carbene as a probable competitive route. On other hand, carbenes produced via H-transfer processes (reaction type 5) can undergo conversion to the lowest energy triplet as well. Generally, singlet/triplet intersystem crossings can be important routes for pyrolysis and combustion processes and the role of these types of the reactions has to be investigated further. The GRRM strategy can be used to determine the structures and energies of minimum energy points on the seam of crossing (MESX) between singlet-triplet crossing hypersurfaces,<sup>58,59</sup> and results of such studies will be reported elsewhere.

### 3.10: Reaction Type 10: Bimolecular H-atom Abstractions from Closed-Shell species

Bimolecular H-atom abstraction from closed-shell species is the most important reaction type to propagate the chain of radicals. These reactions occur through transition states with energies that are much lower than the energies required to produce radicals via unimolecular reactions or even barrierlessly. The energies of the transition state and products of H-abstraction reactions are correlated to the stability of the radicals involved in the reaction step. The reaction steps that involve energetically stable radicals, such as  $\pi$ -C, have transition states and products with lower energies compared to reaction steps that involve energetically unstable radical species, such as  $R\equiv C$  radicals, which proceed through a barrierless process. For instance, H-abstractions with  $sp^3$ -carbon radicals (such as  $CH_3$ ,  $CH_3CH_2$ ,  $CH_3CH_2CH_2$ , and  $CH_3CHCH_3$ ) proceed with a transition state of about 11-20 kcal/mol, depending on the species involved. H-abstractions with  $sp^2$ -carbon radicals (such as  $CH_2=CH$ ,  $CH_3C=CH_2$ , and  $CH_3CH=CH$ ) proceed with a transition state of about 6-14 kcal/mol, depending on the species involved. H-abstractions with  $sp$ -carbon radicals (such as  $CH\equiv C$ ,  $CH_3C\equiv C$ ) usually proceed barrierlessly as noted above. In addition to H-abstractions by carbon-containing radicals from closed-shell species described above, abstractions can also proceed by H-atoms with a transition state of about 8-15 kcal/mol, depending on the species involved. Here, a carbon-containing radical and a hydrogen molecule is

produced. Generally, this reaction type is very important to describe both pyrolysis and oxidation of hydrocarbons.

### **3.11 Reaction Type 11: Bimolecular Radical Recombination Reactions and Reaction Type 12: Bimolecular Disproportionation Reactions**

Bimolecular radical recombination and bimolecular disproportionation are the reactions that terminate a radical chain in pyrolysis of hydrocarbons. Both reaction types proceed through a collision of two radical species through a barrierless process producing closed shell products, with the former recombining to products and the latter being held in a weak complex which then undergoes an H-transfer. These two reaction types are competitive and the relative yield of these processes depends on temperature, pressure and types of radicals involved in the process.<sup>77</sup>

### **3.12 Reaction Type 13: Bimolecular Radical Addition to Unsaturated Bond**

This reaction type includes the reverse reactions described in Reaction Type 6: (unimolecular C-H bond cleavage in radical species) and Reaction Type 7: (unimolecular C-C bond cleavage in radical species). For additions of  $sp^3$ -carbon radicals (such as  $CH_3$ ,  $CH_3CH_2$ ,  $CH_3CH_2CH_2$ , and  $CH_3CHCH_3$ ) to unsaturated hydrocarbons, the transition state is about 7-10 kcal/mol. For additions of  $sp^2$ -carbon radicals (such as  $CH_2=CH$ ,  $CH_3C=CH_2$ , and  $CH_3CH=CH$ ) to unsaturated hydrocarbons, the transition state is about 3-6 kcal/mol. For cyclic  $sp^3$ -carbon radicals (such as  $cyc-CH_2CHCH_2$  and  $cyc-CHCHCH$ ), the transition state is about 4-8 kcal/mol. Cyclic  $sp^2$ -carbon radicals (such as  $cyc-CH_2CCH$ ) can react with unsaturated hydrocarbons via either the C atom or the CH group of  $cyc-CH_2CCH$  with transition states lying about 29 kcal/mol above the energy of the reactants.

### **3.13 Reaction Type 14: Bimolecular Reactions Between Closed Shell Species**

Closed-shell compounds (both  $H_2$  and hydrocarbons) can be added to a double bond of unsaturated hydrocarbons forming saturated hydrocarbons. Reactions occur through transition state with C-C (or H-H) and double C=C bonds breaking and formation of two new C-C (or C-H) bonds. This reaction type includes the reactions that are reverse reactions from reaction type 3 (unimolecular double C-H bond cleavage in closed shell species), reaction type 4 (unimolecular simultaneous C-C and C-H bond cleavage in closed shell species). Another possible route for

interaction between two closed-shell compounds is the reverse reactions for the reaction type 12 (bimolecular disproportionation reactions) forming to reactive radical species. Generally, the contribution of these reactions to secondary processes during pyrolysis or oxidation of hydrocarbons is not expected to be large. However, this reaction type can be important as an initial step of the pyrolysis in some unsaturated hydrocarbons or mixtures of hydrocarbons producing radicals to initiate a radical chain.

### 3.14 Early Stages of Pyrolysis Reactions of C<sub>1</sub>-C<sub>3</sub> Saturated and Unsaturated Hydrocarbons

Although somewhat redundant to data given in Table S1, the early stages of pyrolysis reactions of a variety of C<sub>1</sub>-C<sub>3</sub> saturated and unsaturated hydrocarbons as well as radical species are illustrated in Figures 7-16. In Fig. 7, the pyrolysis of propane shows the most energetically favorable reaction type is C-C bond cleavage leading to methyl and ethyl radicals (reaction t2-2 in table S3). In Fig. 8 for propene pyrolysis, an H-transfer leading to the singlet carbene CH<sub>3</sub>CCH<sub>3</sub> is the energetically favorable reaction type (reaction t5-3 in table S3). In Fig. 9 for ethane and methane pyrolysis, a C-C bond cleavage and a C-H bond cleavage leads to methyl radicals and a hydrogen atom, respectively (reactions t2-1 and t1-1 in table S3, respectively). In Fig. 10 for propyne and allene pyrolysis, H-transfers leads to cyclopropene and the singlet carbene CH<sub>2</sub>CH=CH, respectively (reactions t5-8 and t5-13, respectively). In Fig. 11 for ethylene and acetylene pyrolysis, H-transfers leads to the singlet carbene CH<sub>3</sub>CH and CH<sub>2</sub>=C, respectively (reactions t5-1 and t5-6, respectively). In Fig. 12 for cyclopropane and cyclopropene pyrolysis, C-C bond cleavage followed by an H-transfer leads to propene and propyne, respectively (reactions t2-10 and t2-12, respectively). In Fig. 13 for n-propyl and iso-propyl radical pyrolysis, a beta-scission and a C-H bond cleavage leads to ethylene and a methyl radical (reaction t7-2) or propene (reaction t6-4), respectively. In Fig. 14 for propenyl radical pyrolysis, both CH<sub>2</sub>CH=CH<sub>2</sub> and CH<sub>3</sub>CH=CH isomerize to CH<sub>3</sub>C=CH<sub>2</sub> (reactions t8-3 and t8-5, respectively), which then leads to propyne and an H atom by a C-H bond cleavage (reaction t8-11). In Fig. 15 for ethyl, ethenyl and methyl radicals, C-H bond cleavages leads to ethylene, acetylene, and singlet methyl carbene and an H atom (reactions t6-2, t6-15, and t6-1, respectively). In Fig. 16 for cyclopropyl and cyclopropenyl radicals, a C-C bond cleavage leads

to a propenyl radical  $\text{CH}_2\text{CH}=\text{CH}_2$  and propynyl radical  $\text{CH}_2\text{C}\equiv\text{C}$ , respectively (reactions t7-15 and t7-16, respectively).

--- Fig. 7 ---

--- Fig. 8 ---

--- Fig. 9 ---

--- Fig. 10 ---

--- Fig. 11 ---

--- Fig. 12 ---

--- Fig. 13 ---

--- Fig. 14 ---

--- Fig. 15 ---

--- Fig. 16 ---

#### 4. Conclusions

One of the major goals in pyrolysis and combustion modeling is the construction of a detailed kinetic model entirely from first principles. This study is the first of two fundamental steps in fully understanding the pyrolysis of  $\text{C}_1\text{-C}_3$  hydrocarbons from first principles. The first is to establish a systematic mapping at a consistent level of theory of all of the possible reaction types and channels and compute barriers and energies. The second is using the data provided in this article in future first principle kinetic studies in developing a reliable detailed kinetic model for the pyrolysis of these compounds.

The GRRM strategy at the UM06-2x/6-31g\* level of theory was employed for an ab initio global investigation of the topology of potential energy surfaces for species and reactions considered in this study. Geometry refinements were then made at the UM06-2X/cc-pVTZ level of theory. All of energies of reactants, products, and transition states are calculated at the UCCSD(T)-F12b/cc-pVTZ//UM06-2X/cc-pVTZ + ZPE(UM06-2X/cc-pVTZ level of theory. Standard enthalpies are calculated at the UCCSD(T)-F12b/cc-pVTZ//UM06-2x/cc-pVTZ + UM06-2X/cc-pVTZ for the entropy correction level of theory. The comparison of the calculated enthalpies of reactions with 41 available experimental values from NIST database gives the root mean square error of 0.8 kcal/mol.

The reaction network investigated in this study is generated on the base of 25 species ( $C_3$  hydrocarbons radicals and singlet closed shell species,  $H_2$  and  $H$ ) and consists of 823 reactions that are classified into 14 reaction types. Analysis of the energies of the reactions from different reaction types reveals the following. For unimolecular decomposition of closed-shell  $C_1$ - $C_3$  hydrocarbons, C-C bond cleavages are the energetically favorable reaction types for alkanes. Alkenes and alkynes can either undergo bimolecular disproportionation to form radicals, hydrogen transfers to form carbenes, or intersystem crossing to access the triplet potential energy surface. Therefore, several reaction types for decomposition of alkenes and alkynes are competitive and should be considered for construction of detailed kinetic models.

Additional studies for the reactions of  $C_1$ - $C_3$  hydrocarbons on the triplet and excited singlet potential energy surface as well as reactions that involved carbene and carbyne species have to be performed to further investigate the role of these factors in the pyrolysis of hydrocarbons. All bimolecular reaction types involving radicals as a reactant are energetically favorable in comparison with unimolecular reactions and are important for propagation and termination of the radical chain. The data reported in this article can be used for first principle calculations of kinetic constants and for a subsequent modeling of evolution of the species in pyrolysis and oxidation of hydrocarbons. The reactions involved in this study can be used for the pyrolysis of larger hydrocarbons or less studied systems, where the GRRM strategy can also be employed.

### Supporting Information

Table S1 gives Optimized Cartesian coordinates, energies at the UM06-2X/cc-pVTZ and UCCSD(T)-F12/cc-pVTZ//UM06-2X/cc-pVTZ level of theory, ZPE(UM06-2X/cc-pVTZ), and vibrational frequencies of all  $C_1$ - $C_3$  species and all reaction steps included in this study. Table S2 gives species and standard heats of formation energies of NIST values obtained from the Gas-phase thermochemistry data in the Webbook of the National Institute of Standards and Technology (NIST) and the Active Thermochemical Tables (ATcT). Table S3 gives reaction steps, reaction barrier heights (TS), energies (with ZPE corrections), and enthalpies of reactions are calculated at the UCCSD(T)-F12b/cc-pVTZ//UM06-2X/cc-pVTZ + ZPE(UM06-2X/cc-pVTZ) level of theory (in kcal/mol). Experimental values are obtained from the NIST database.

### Acknowledgement

The authors are grateful to Profs. Oscar N. Ventura, Hai Wang, Ronald K. Hanson, William G. Green and Yuhguang Ju for discussions. The work at Emory is in part supported by a subcontract at Emory University of the AFOSR BRI grant FA9550-12-1-0472. The work in Japan is in part supported by grants from Japan Society for the Promotion of Science (Grants-in-Aid for Scientific Research <KAKENHI> No. 24245005 at Kyoto University and No. 23685004 at Hokkaido University). The Computer resources at the Research Center of Computer Science (RCCS) at the Institute for Molecular Science are also acknowledged.

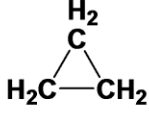
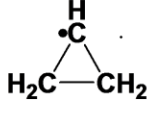
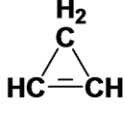
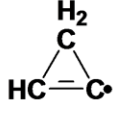
C <sub>3</sub>	<b>C<sub>3</sub>H<sub>8</sub></b> CH <sub>3</sub> CH <sub>2</sub> CH <sub>3</sub>	<b>C<sub>3</sub>H<sub>7</sub></b> CH <sub>3</sub> CH <sub>2</sub> ĊH <sub>2</sub> CH <sub>3</sub> ĊHCH <sub>3</sub>	<b>C<sub>3</sub>H<sub>6</sub></b> CH <sub>3</sub> CH=CH <sub>2</sub> 	<b>C<sub>3</sub>H<sub>5</sub></b> CH <sub>3</sub> CH=ĊH CH <sub>3</sub> Ċ=CH <sub>2</sub> ĊH <sub>2</sub> CH=CH <sub>2</sub> 	<b>C<sub>3</sub>H<sub>4</sub></b> CH <sub>2</sub> =C=CH <sub>2</sub> CH <sub>3</sub> C≡CH 	<b>C<sub>3</sub>H<sub>3</sub></b> CH <sub>2</sub> =C=ĊH CH <sub>3</sub> C≡Ċ 
	<b>C<sub>2</sub>H<sub>6</sub></b> CH <sub>3</sub> CH <sub>3</sub>	<b>C<sub>2</sub>H<sub>5</sub></b> CH <sub>3</sub> ĊH <sub>2</sub>	<b>C<sub>2</sub>H<sub>4</sub></b> CH <sub>2</sub> =CH <sub>2</sub>	<b>C<sub>2</sub>H<sub>3</sub></b> CH <sub>2</sub> =ĊH	<b>C<sub>2</sub>H<sub>2</sub></b> CH≡CH	<b>C<sub>2</sub>H</b> CH≡Ċ
	<b>C<sub>1</sub></b>	<b>CH<sub>4</sub></b> CH <sub>4</sub>	<b>CH<sub>3</sub></b> ĊH <sub>3</sub>			

Fig. 1. C<sub>1</sub>-C<sub>3</sub> species considered in the present study.

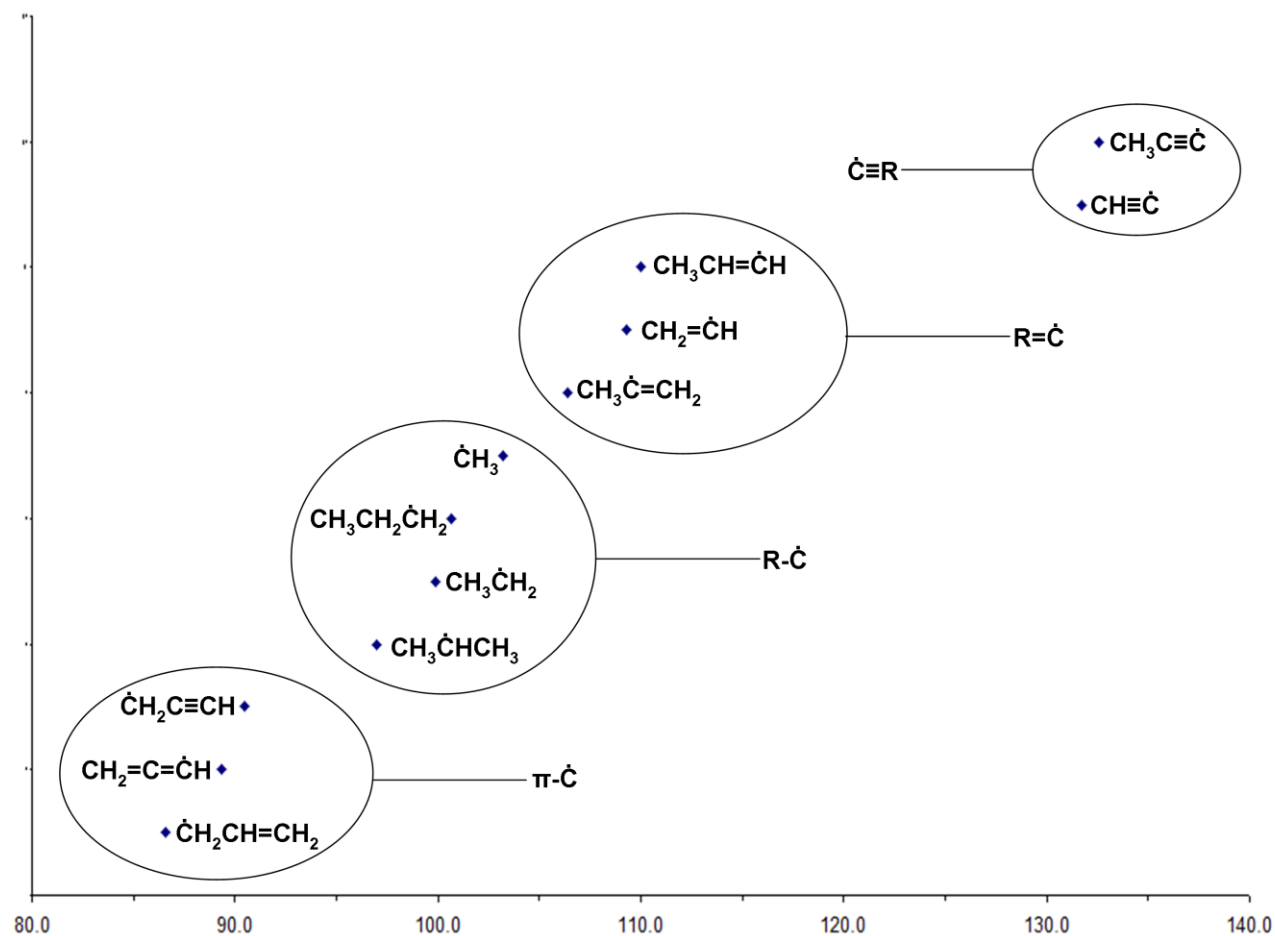


Fig. 2. The C-H bond dissociation energies (in kcal/mol) of closed shell molecules producing radical species. All stationary points were optimized at the UM06-2X/cc-pVTZ level, and energies calculated at the UCCSD(T)-F12b/cc-pVTZ//UM06-2X/cc-pVTZ + ZPE(UM06-2X/cc-pVTZ) level.

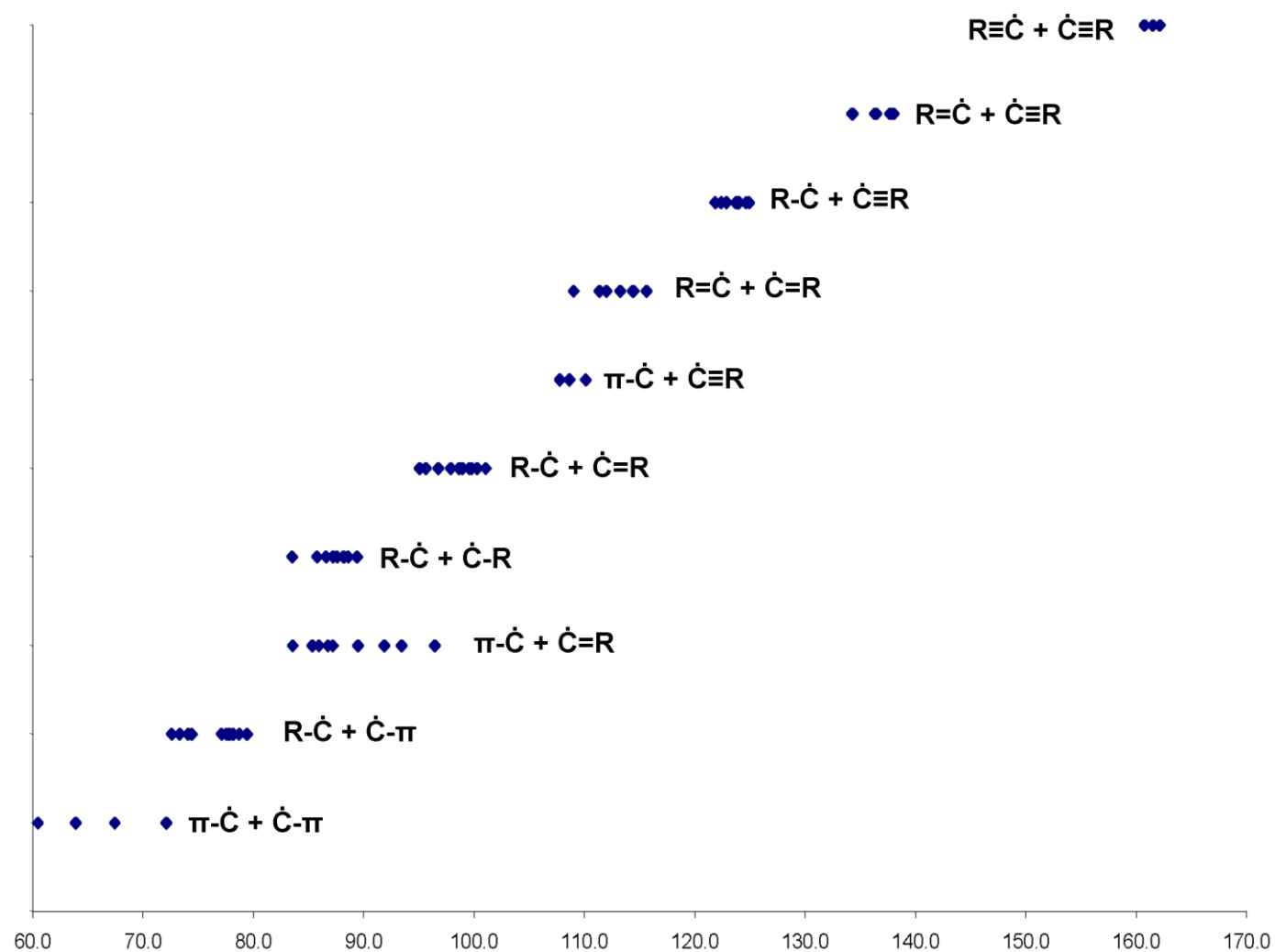


Fig. 3. The C-C bond dissociation energies (in kcal/mol) of closed shell molecules producing radical species. See Fig. 2 for details.

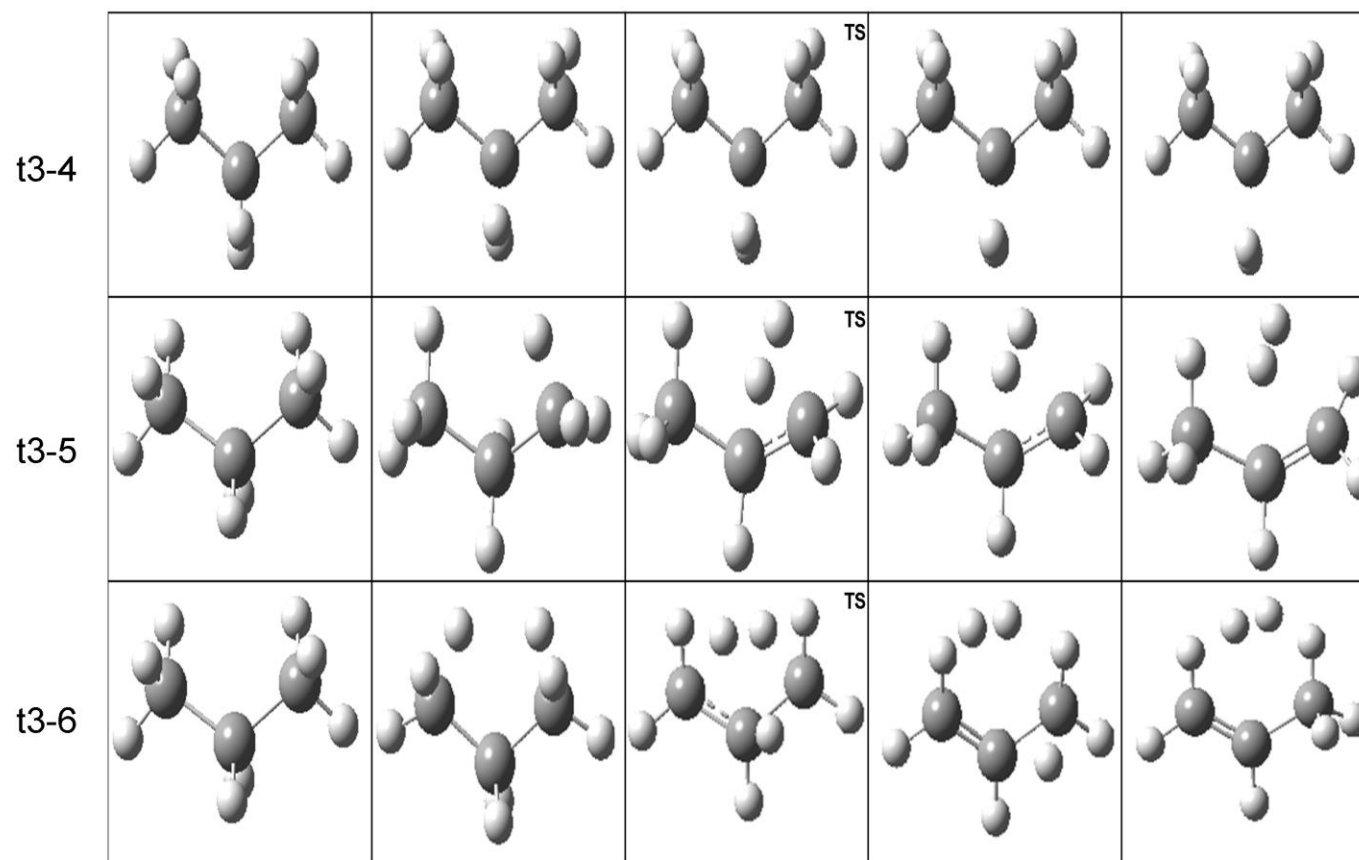


Fig.4. Snapshots along the minimum energy path for reactions t3-4, t3-5, t3-6 (Reaction Type 3).

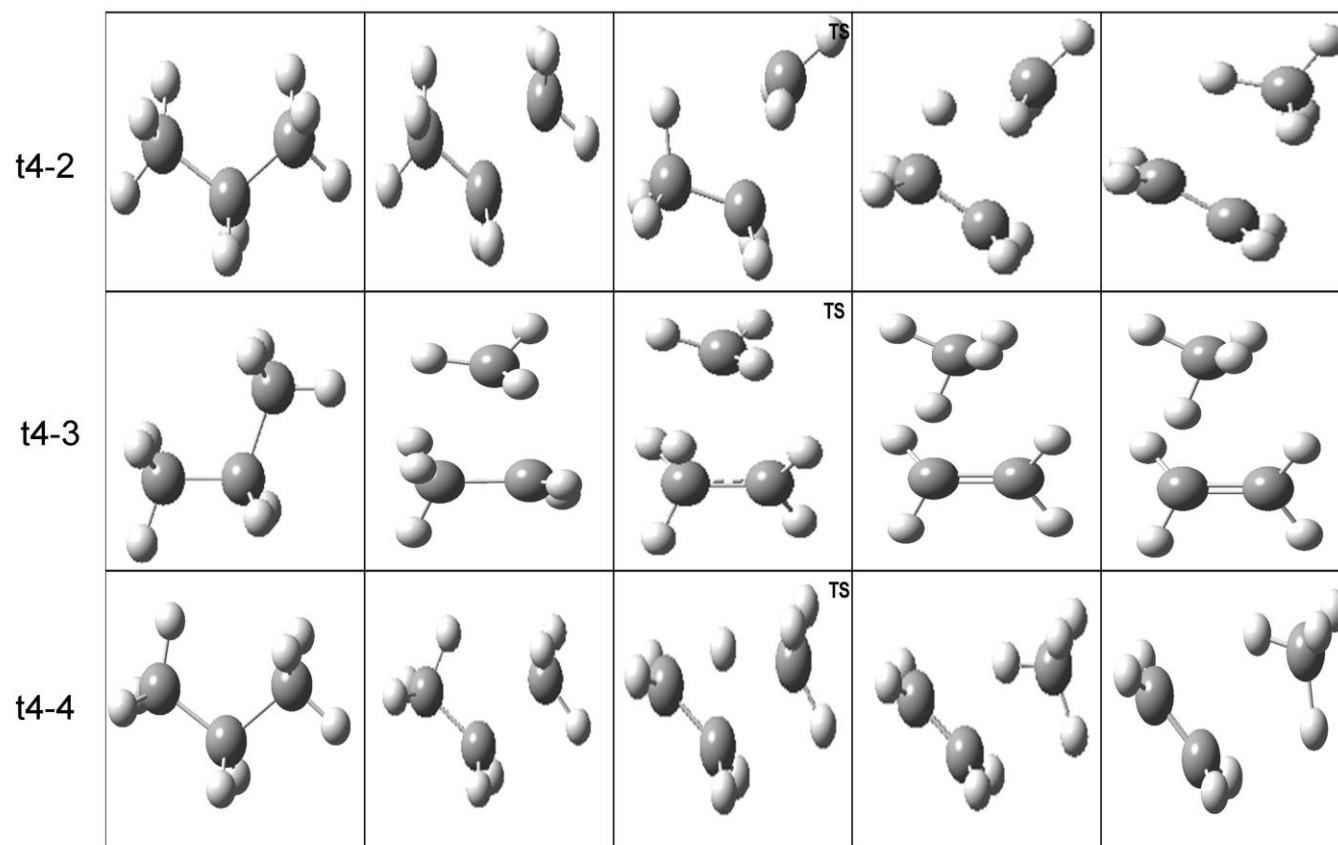


Fig. 5. Snapshots along the minimum energy path for reactions t4-2, t4-3, t4-4 (Reaction Type 4).

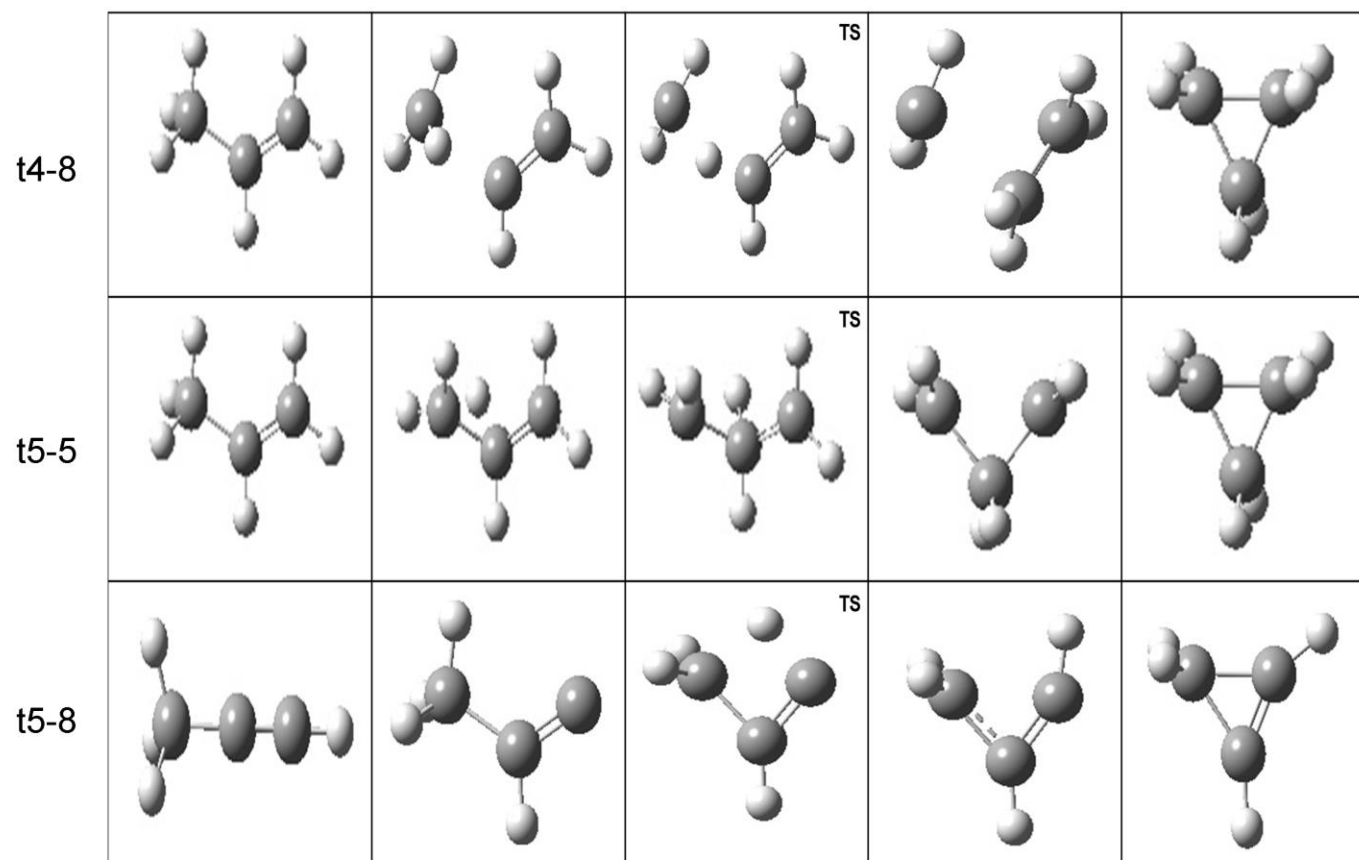


Fig. 6. Snapshots along the minimum energy path for reactions t4-8, t5-5, t5-8 (Reaction Type 4 and 5).

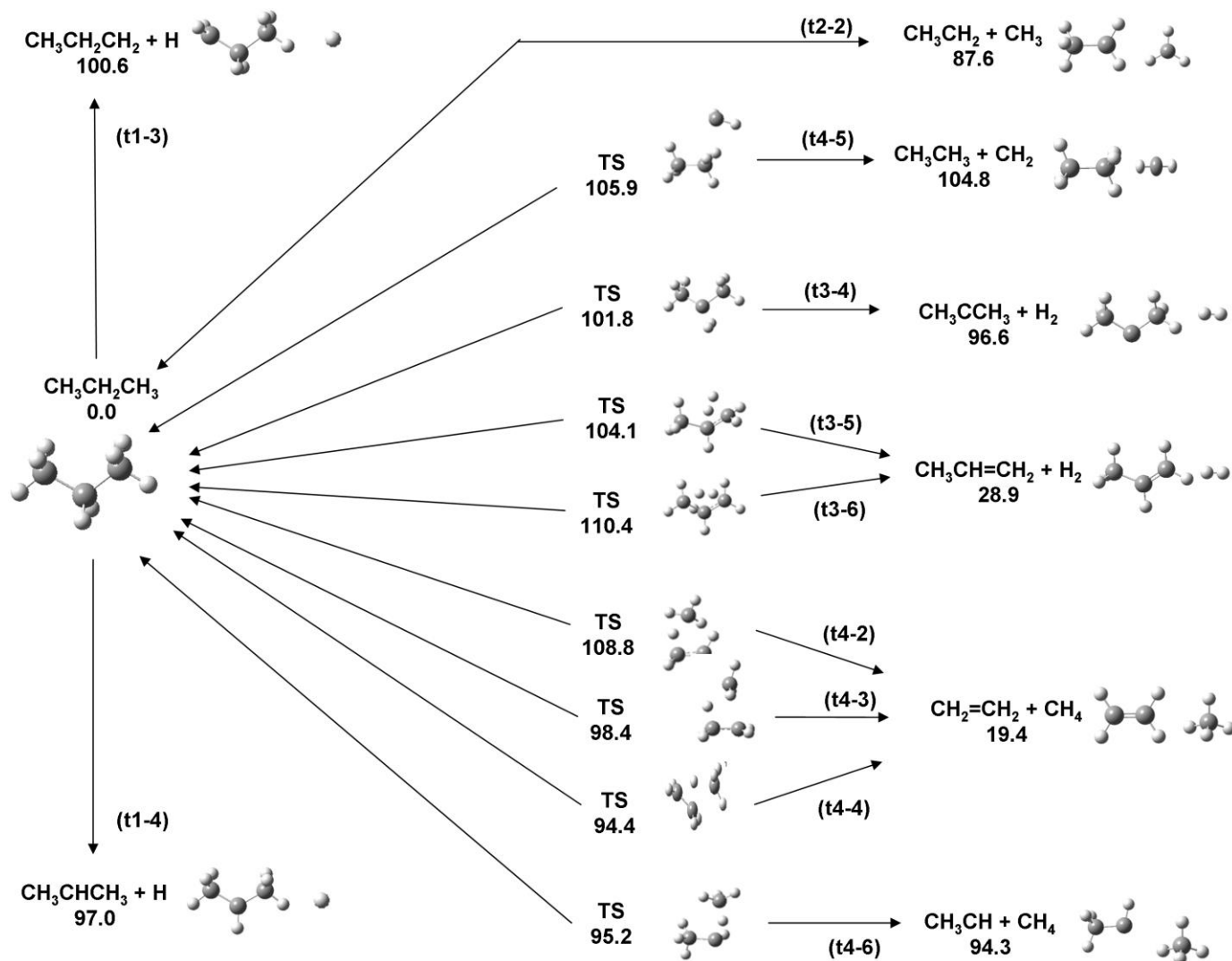


Fig. 7. Reaction steps involved in the unimolecular decomposition of propane. See Fig. 2 for details.

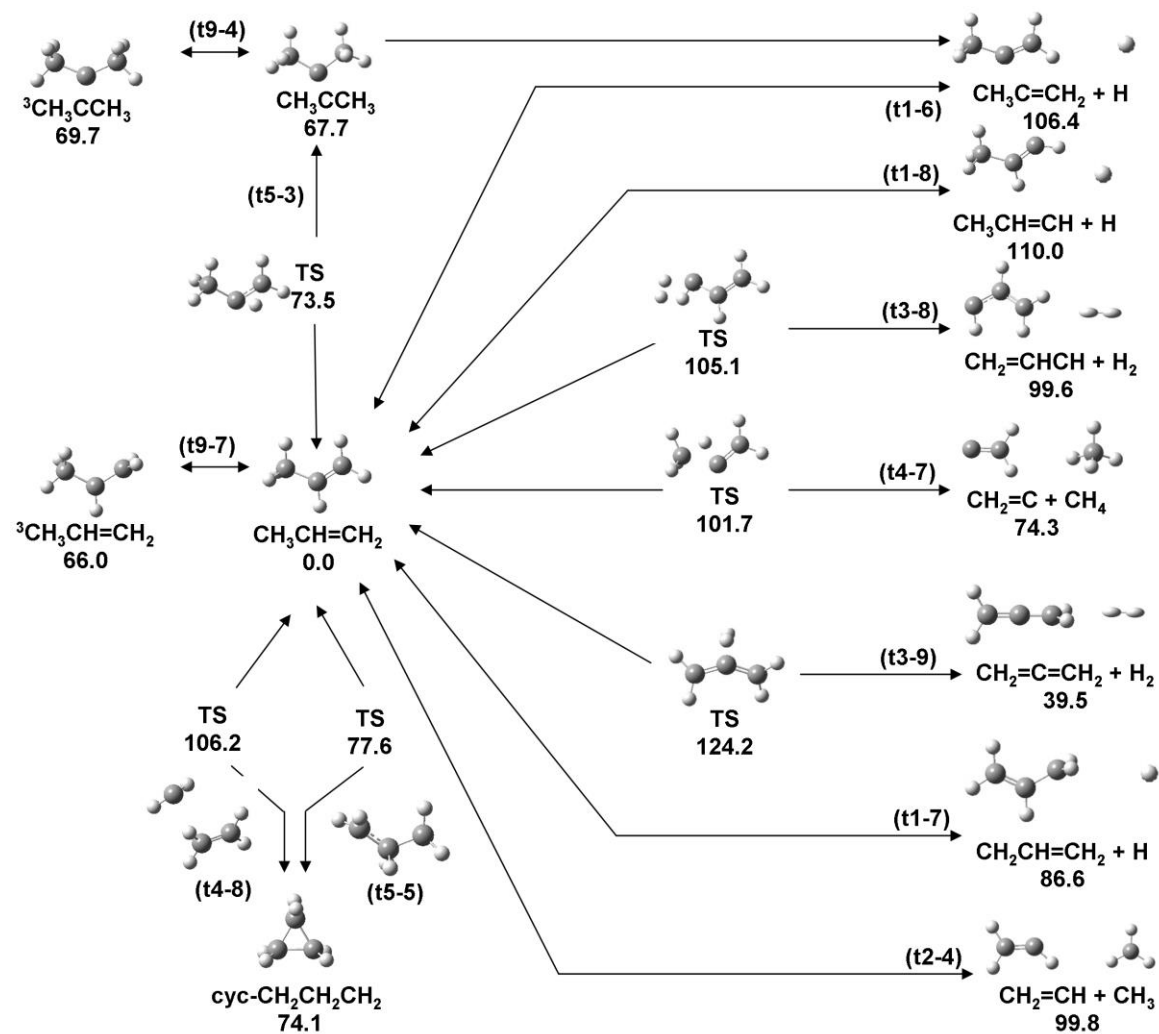


Fig. 8. Reaction steps involved in the unimolecular decomposition and isomerization of propene. See Fig. 2 for details.

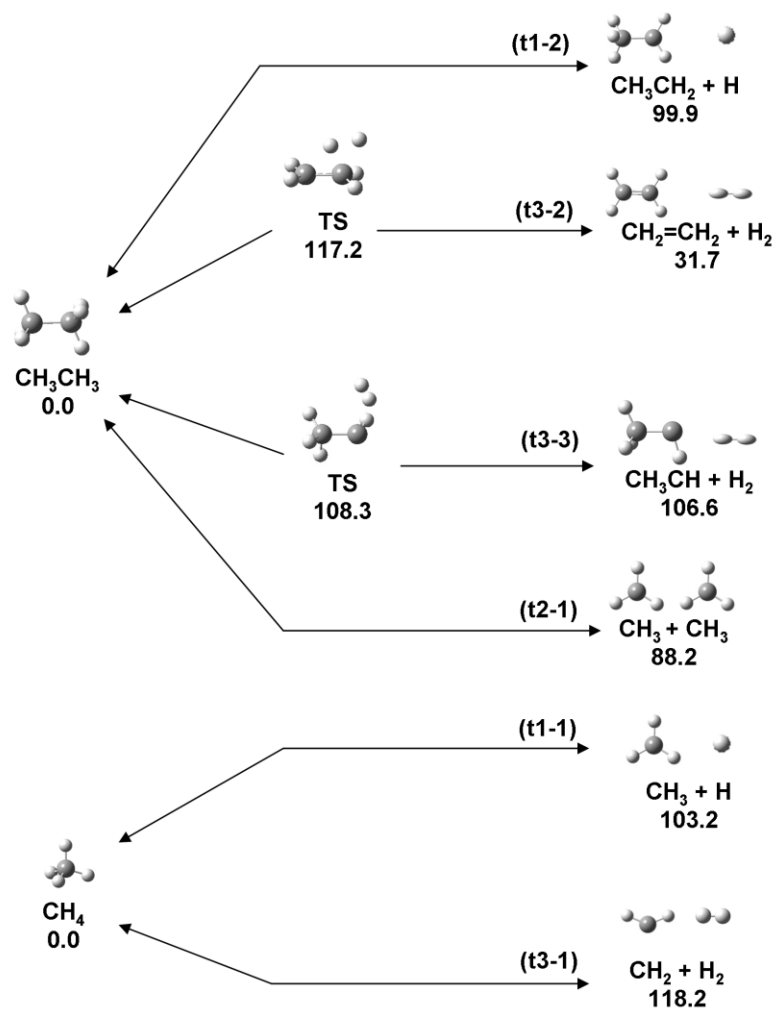


Fig. 9. Reaction steps involved in the unimolecular decomposition of ethane and methane. See Fig. 2 for details.

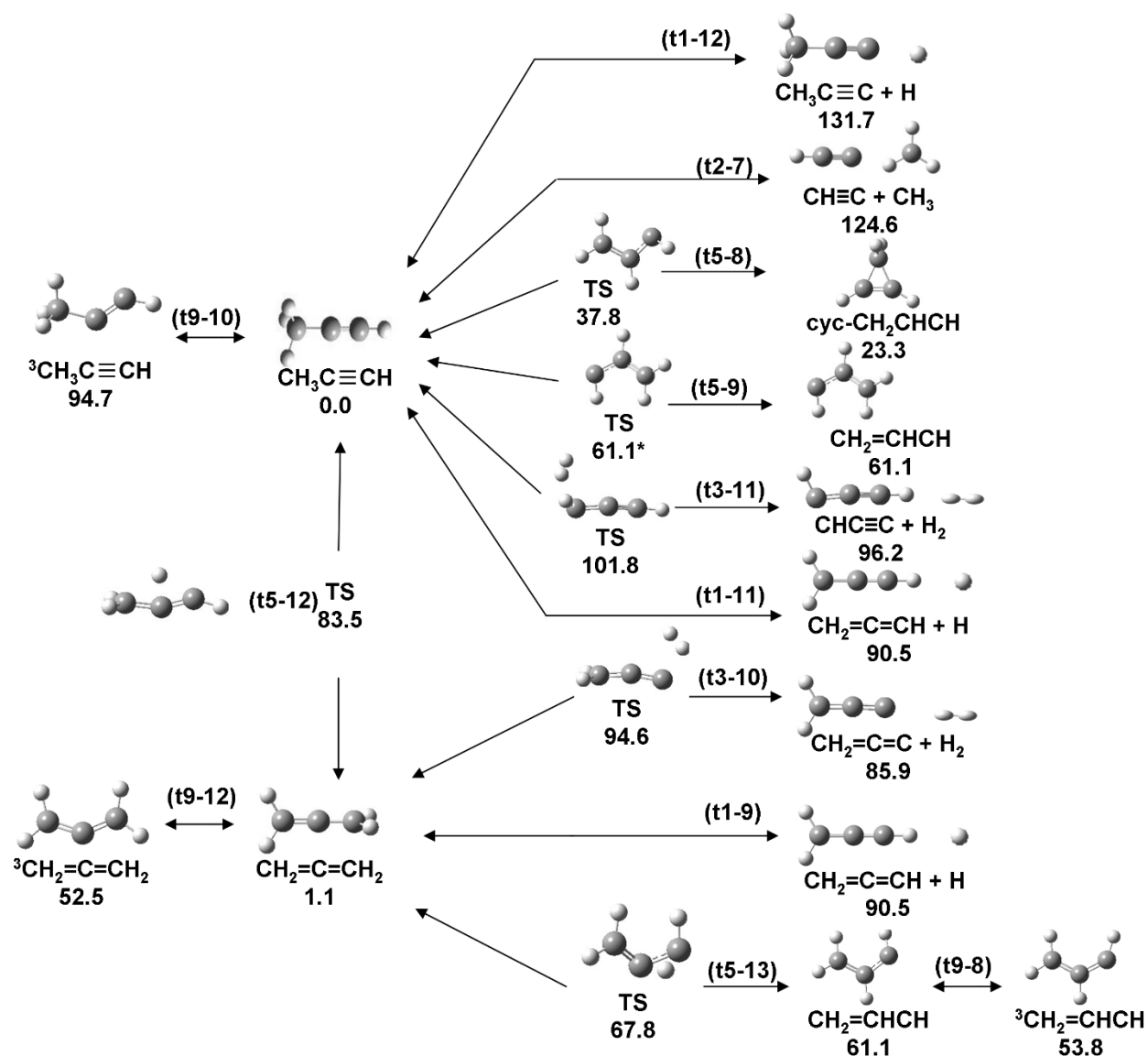


Fig. 10. Reaction steps involved in the unimolecular decomposition and isomerization of allene and propyne. See Fig. 2 for details.

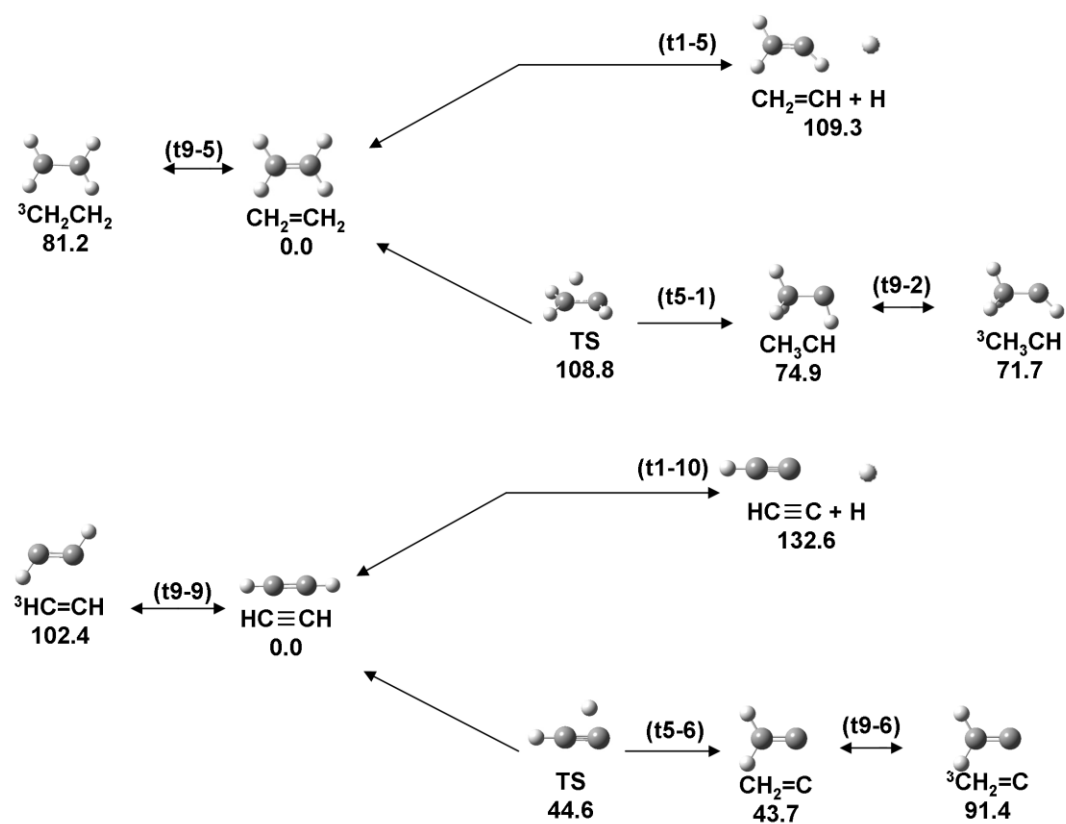


Fig. 11. Reaction steps involved in the unimolecular decomposition and isomerization of ethylene and acetylene. See Fig. 2 for details.

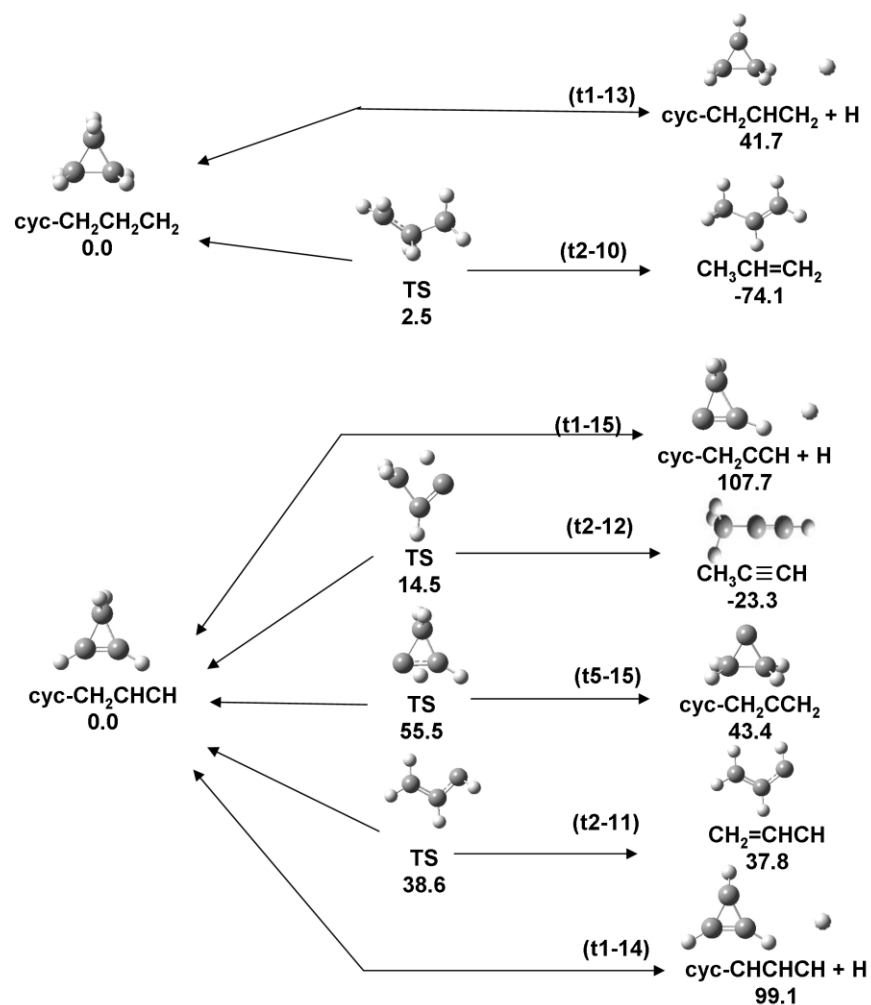


Fig. 12. Reaction steps involved in the unimolecular decomposition and isomerization of cyclopropane and cyclopropene. See Fig. 2 for details.

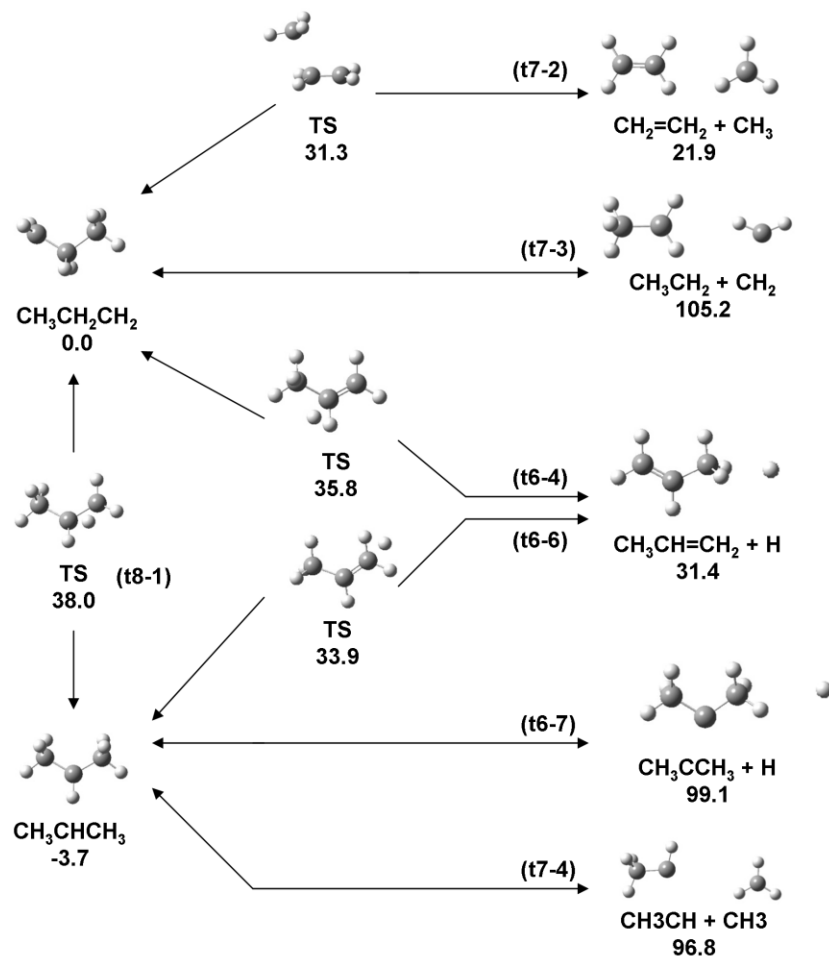


Fig. 13. Reaction steps involved in the unimolecular decomposition and isomerization of n-propyl radical and iso-propyl radical. See Fig. 2 for details.

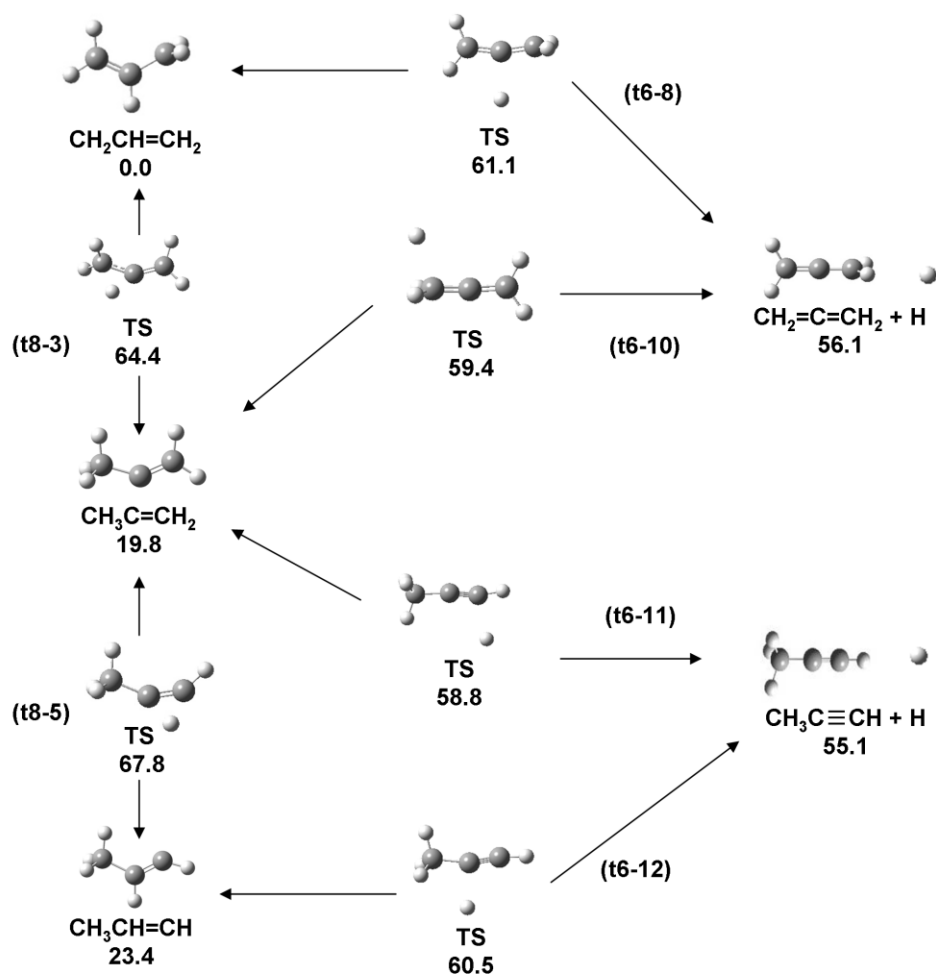


Fig. 14. Reaction steps involved in the unimolecular decomposition and isomerization of propenyl radical. See Fig. 2 for details.

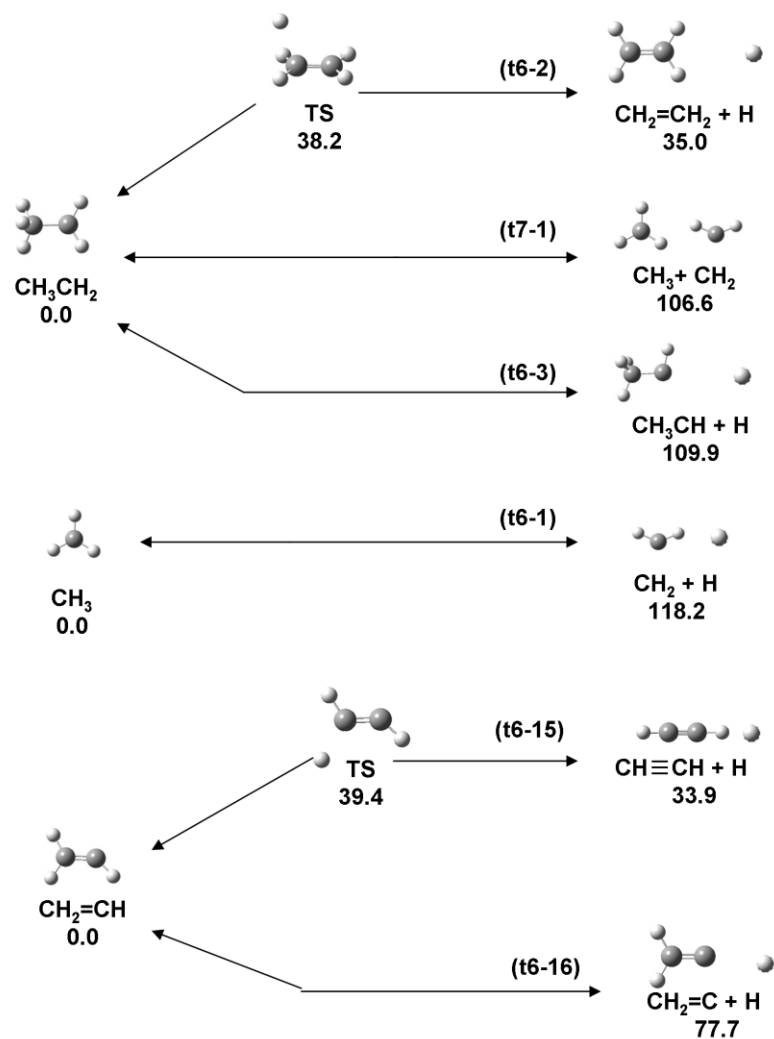


Fig. 15. Reaction steps involved in the unimolecular decomposition of ethyl, methyl, and ethenyl radicals. A See Fig. 2 for details.

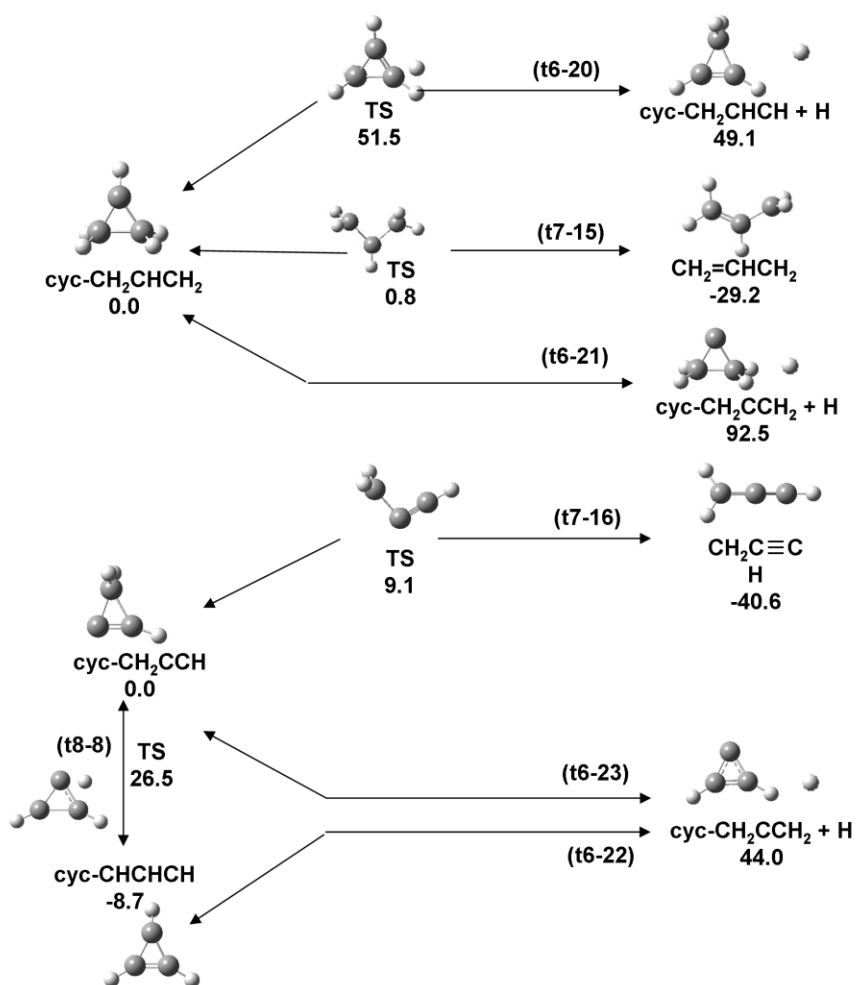


Fig. 16. Reaction steps involved in the unimolecular decomposition and isomerization of cyclopropyl and cyclopropenyl radicals. See Fig. 2 for details.



**References.**

1. J.C. Guibet, Fuels and engines, Publications de l'Institut Français du Pétrole, Editions Technip, Paris, 1999.
2. J.T. Farrell, N.P. Cernansky, F.L. Dryer, D.G. Friend, C.A. Hergart, C.K. Law, R.M. McDavid, C.J. Mueller, A.K. Patel, H. Pitsch, *SAE Intern.*, 2007.
3. D.F. Davidson, R.K. Hanson, *Shock Waves*, 2009, **19**, 271-283.
4. D.F. Davidson, M.A. Oehlschlaeger, R.K. Hanson, *Proc. Combust. Inst.*, 2007, **31**, 321-328.
5. R.K. Hanson, G.A. Pang, S. Chakraborty, W. Ren, S.K. Wang, D.F. Davidson, *Combust. Flame*, 2013, **160**, 1550-1558.
6. I. Stranic, D.F. Davidson, R.K. Hanson, *Chem. Phys. Lett.*, 2013, **584**, 18-23.
7. R. Hanson, D. Davidson, *Prog. Energ. Combust*, 2014, **44**, 103-114.
8. E.E. Dames, K.-Y. Lam, D.F. Davidson, R.K. Hanson, *Combust. Flame*, 2013, **160**, 2669-2675
9. Y. Zhu, D. Davidson, R. Hanson, *Combust. Flame*, 2014, **161**, 371-383.
10. S. Li, D.F. Davidson, R.K. Hanson, N.J. Labbe, P.R. Westmoreland, P. Oßwald, K. Kohse-Höinghaus, *Combust. Flame*, 2013, **160**, 1559-1571.
11. J.F. Griffiths, J.A. Barnard, *Flame and combustion*, 3rd ed., Springer, 1998.
12. J. Warnatz, U. Maas, R.W. Dibble, *Combustion: physical and chemical fundamentals, modeling and simulation, experiments, pollutant formation*, 4th ed., Springer, 2006.
13. A.S. Tomlin, T. Turanyi, M.J. Pilling, *Mathematical tools for the construction, investigation and reduction of combustion mechanisms Low-temperature combustion and autoignition*, Elsevier, 1997, 293-437.
14. C.K. Westbrook, Y. Mizobuchi, T.J. Poinot, P.J. Smith, J. Warnatz, *Proc. Combust. Inst.*, 2005, **30**, 125-157.
15. J. Buckmaster, P. Clavin, A. Linan, M. Matalon, N. Peters, G. Sivashinsky, F.A. Williams, *Proc. Combust. Inst.*, 2005, **30**, 1-19.
16. C.K. Westbrook, W.J. Pitz, O. Herbinet, H.J. Curran, E.J. Silke, *Combust. Flame*, 2009, **156**, 181-199.
17. J.M. Simmie, *Prog. Energ. Combust.*, 2003, **29**, 599-634.
18. F. Battin-Leclerc, E. Blurock, R. Bounaceur, R. Fournet, P.A. Glaude, O. Herbinet, B. Sirjean, V. Warth, *Chem. Soc. Rev.*, 2011, **40**, 4762-4782.
19. C.K. Westbrook, F.L. Dryer, *Prog. Energ. Combust.*, 1984, **10**, 1-57.
20. L.B. Harding, S.J. Klippenstein, *J. Phys. Chem. Lett.*, 2010, **1**, 3016-3020.
21. R. Sivaramakrishnan, M.-C. Su, J. Michael, S. Klippenstein, L. Harding, B. Ruscic, *J. Phys. Chem. A*, 2011, **115**, 3366-3379.
22. R. Sivaramakrishnan, J. Michael, A. Wagner, R. Dawes, A. Jasper, L. Harding, Y. Georgievskii, S. Klippenstein, *Combust. Flame*, 2011, **158**, 618-632.
23. S.W. Benson, *Thermochemical kinetics*, 2nd ed., Wiley, New York, 1976.
24. R. Sumathi, H.H. Carstensen, W.H. Green, *J. Phys. Chem. A*, 2001, **105**, 6910-6925.
25. M. Saeys, M.F. Reyniers, V. Van Speybroeck, M. Waroquier, G.B. Marin, *Chem. Phys. Chem.*, 2006, **7**, 188-199.
26. M.K. Sabbe, F. De Vleeschouwer, M.F. Reyniers, M. Waroquier, G.B. Marin, *J. Phys. Chem. A*, 2008, **112**, 12235-12251.
27. L.J. Broadbelt, J. Pfaendtner, *AIChE*, 2005, 2112-2121.
28. H.-H. Carstensen, A.M. Dean, *J. Phys. Chem. A*, 2009, **113**, 367-380.
29. R. Vinu, L.J. Broadbelt, *An. Rev. Chem. Biomol. Eng.*, 2012, **3**, 29-54.

30. J.R. Barker, *J. Chem. Kinet.*, 2009, **41**, 748-763.
31. J.R. Barker, L.M. Yoder, K.D. King, *J. Phys. Chem. A*, 2001, **105**, 796-809.
32. J. Troe, *Berichte der Bunsengesellschaft für physikalische Chemie*, 1973, **77**, 665-674.
33. V. Bernshtein, I. Oref, *J. Phys. Chem.*, 1993, **97**, 6830-6834.
34. D.M. Golden, J.R. Barker, *Combust. Flame*, 2011, **158**, 602-617.
35. M. Frenklach, H. Wang, M.J. Rabinowitz, *Prog. Energ. Combust.*, 1992, **18**, 47-73.
36. M. Frenklach, A. Packard, R. Feeley, *Comprehensive Chemical Kinetics*, 2007, **42**, 243-291.
37. T. Russi, A. Packard, R. Feeley, M. Frenklach, *J. Phys. Chem. A*, 2008, **112**, 2579-2588.
38. G.P. Smith, D.M. Golden, M. Frenklach, N.W. Moriarty, B. Eiteneer, M. Goldenberg, C.T. Bowman, R.K. Hanson, S. Song, W.C. Gardiner Jr., V.V. Lissianski, Z. Qin, [http://www.me.berkeley.edu/gri\\_mech/](http://www.me.berkeley.edu/gri_mech/).
39. M. Saeys, M.F. Reyniers, G.B. Marin, V. Van Speybroeck, M. Waroquier, *J. Phys. Chem. A*, 2003, **107**, 9147-9159.
40. P. Vansteenkiste, V. Van Speybroeck, G.B. Marin, M. Waroquier, *J. Phys. Chem. A*, 2003, **107**, 3139-3145.
41. A.G. Vandeputte, M.K. Sabbe, M.F. Reyniers, V. Van Speybroeck, M. Waroquier, G.B. Marin, *J. Phys. Chem. A*, 2007, **111**, 11771-11786.
42. L.B. Harding, Y. Georgievskii, S.J. Klippenstein, *J. Phys. Chem. A*, 2005, **109**, 4646-4656.
43. S.J. Klippenstein, Y. Georgievskii, L.B. Harding, *Phys. Chem. Chem. Phys.*, 2006, **8**, 1133-1147.
44. A. Fernández-Ramos, J.A. Miller, S.J. Klippenstein, D.G. Truhlar, *Chem. Rev.*, 2006, **106**, 4518-4584.
45. M.J. Pilling, S.H. Robertson, *Ann. Rev. Phys. Chem.*, 2003, **54**, 245-275.
46. J.A. Miller, S.J. Klippenstein, *J. Phys. Chem. A*, 2006, **110**, 10528-10544.
47. S.J. Klippenstein, V.S. Pande, D.G. Truhlar, *J. Am. Chem. Soc.*, 2014, **136**, 528-546.
48. M.E. Segovia, K. Irving, O.N. Ventura, *Theor. Chem. Acc.*, 2013, **132**, 1-18.
49. W.J. Sunand, M. Saeys, *Aiche J*, 2011, **57**, 2458-2471.
50. L.J. Broadbelt, S.M. Stark, M.T. Klein, *I&E Chem. Res.*, 1994, **33**, 790-799.
51. M.J. De Witt, D.J. Dooling, L.J. Broadbelt, *I&E Chem. Res.*, 2000, **39**, 2228-2237.
52. K.M. Van Geem, M.F. Reyniers, G.B. Marin, J. Song, W.H. Green, D.M. Matheu, *Aiche J*, 2006, **52**, 718-730.
53. W.H. Green, J.W. Allen, B.A. Buesser, R.W. Ashcraft, G.J. Beran, C.A. Class, C. Gao, C.F. Goldsmith, M.R. Harper, A. Jalan, M. Keceli, G.R. Magoon, D.M. Matheu, S.S. Merchant, J.D. Mo, S. Petway, S. Raman, S. Sharma, J. Song, Y. Suleymanov, K.M. Van Geem, J. Wen, R.H. West, A. Wong, H.-W. Wong, P.E. Yelvington, N. Yee, J. Yu, <http://rmg.sourceforge.net/>, 2013.
54. S. Maeda, K. Morokuma, *J. Chem. Theor. Comput.*, 2011, **7**, 2335-2345.
55. S. Maeda, R. Saito, K. Morokuma, *J. Phys. Chem. Lett.*, 2011, **2**, 852-857.
56. S. Maeda, K. Ohno, K. Morokuma, *Phys. Chem. Chem. Phys.*, 2013, **15**, 3683-3701.
57. S. Maeda, T. Taketsugu, K. Morokuma, *J. Comp. Chem.*, 2014, **35**, 166-173.
58. S. Maeda, K. Ohno, K. Morokuma, *J. Phys. Chem. A*, 2009, **113**, 1704-1710.
59. F. Battin-Leclerc, *Prog. Energ. Combust.*, 2008, **34**, 440-498.
60. M.A. Oehlschlaeger, D.F. Davidson, R.K. Hanson, *Proc. Combust. Inst.*, 2005, **30**, 1119-1127.
61. Y. Zhao, D.G. Truhlar, *Theor. Chem. Acc.*, 2008, **120**, 215-241.
62. T.B. Adler, G. Knizia, H.-J. Werner, *J. Chem. Phys.*, 2007, **127**, 221106.
63. G. Knizia, T.B. Adler, H.-J. Werner, *J. Chem. Phys.*, 2009, **130**, 054104.

64. M.J. Frisch, G.W. Trucks, H.B. Schlegel, G.E. Scuseria, M.A. Robb, J.R. Cheeseman, G. Scalmani, V. Barone, B. Mennucci, G.A. Petersson, H. Nakatsuji, M. Caricato, X. Li, H.P. Hratchian, A.F. Izmaylov, J. Bloino, G. Zheng, J.L. Sonnenberg, M. Hada, M. Ehara, K. Toyota, R. Fukuda, J. Hasegawa, M. Ishida, T. Nakajima, Y. Honda, O. Kitao, H. Nakai, T. Vreven, J.A. Montgomery Jr., J.E. Peralta, F. Ogliaro, M.J. Bearpark, J. Heyd, E.N. Brothers, K.N. Kudin, V.N. Staroverov, R. Kobayashi, J. Normand, K. Raghavachari, A.P. Rendell, J.C. Burant, S.S. Iyengar, J. Tomasi, M. Cossi, N. Rega, N.J. Millam, M. Klene, J.E. Knox, J.B. Cross, V. Bakken, C. Adamo, J. Jaramillo, R. Gomperts, R.E. Stratmann, O. Yazyev, A.J. Austin, R. Cammi, C. Pomelli, J.W. Ochterski, R.L. Martin, K. Morokuma, V.G. Zakrzewski, G.A. Voth, P. Salvador, J.J. Dannenberg, S. Dapprich, A.D. Daniels, Ö. Farkas, J.B. Foresman, J.V. Ortiz, J. Cioslowski, D.J. Fox, Gaussian, Inc., Wallingford, CT, USA, 2009.
65. H.-J. Werner, P.J. Knowles, G. Knizia, F.R. Manby, M. Schütz, Wiley Interdisciplinary Reviews: Computational Molecular Science, 2012, **2**, 242-253.
66. <http://webbook.nist.gov/chemistry/>.
67. K.-N. Fan, Z.-H. Li, W.-N. Wang, H.-H. Huang, W. Huang, *Chem. Phys. Lett.*, 1997, **277**, 257-263.
68. R. Duran, V. Amorebieta, A. Colussi, *J. Phys. Chem.*, 1988, **92**, 636-640.
69. E. Ghibaudi, A. Colussi, *J. Phys. Chem.*, 1988, **92**, 5839-5842.
70. J.H. Kiefer, *Int. J. Chem. Kinet.*, 1993, **25**, 215-219.
71. M. Back, *Can. J. Chem.*, 1971, **49**, 2199-2204.
72. G. Minkoff, *Can. J. Chem.*, 1958, **36**, 131-136.
73. M. Ahmed, D.S. Peterka, A.G. Suits, *J. Chem. Phys.*, 1999, **110**, 4248-4253.
74. H. Curran, P. Gaffuri, W.J. Pitz, C.K. Westbrook, *Combust. Flame*, 1998, **114**, 149-177.
75. H.J. Curran, P. Gaffuri, W. Pitz, C. Westbrook, *Combust. Flame*, 2002, **129**, 253-280.
76. Y. Qu, K. Su, X. Wang, Y. Liu, Q. Zeng, L. Cheng, L. Zhang, *J. Comp. Chem.*, 2010, **31**, 1421-1442.
77. R.D. Kelley, R. Klein, *J. Phys. Chem.*, 1974, **78**, 1586-1595.
78. K. M. Ervin, J. Ho, W. C. Lineberger, *J. Chem. Phys.* 1989, **91**, 5974-5992.
79. N. Chang, M. Shen, C. Yu, *J. Chem. Phys.*, 1997, **106**, 3237-3242.
80. B. Ruscic, Active Thermochemical Tables (ATcT) values based on ver. 1.112 of the Thermochemical Network (2013); available at ATcT.anl.gov
81. A. M. Mebel, K. Morokuma, M. C. Lin, *J. Chem. Phys.*, 1995, **103**, 7414-7421.
82. R. S. Zhu, Z. F. Xu, M. C. Lin. *J. Chem. Phys.*, 2004, **120**, 6566-6573.